# 7

# Sensors for rendezvous navigation

The subject of this chapter is the discussion of the measurement principles of sensors for relative navigation, required in the far and close range rendezvous phases to measure the relative state between the chaser and target vehicles. In the rendezvous phases proper (see figure 2.1), the accuracy of absolute navigation will no longer be sufficient. With one exception, sensor principles for absolute navigation will not be discussed here, since the measurement principles for absolute attitude and absolute position for spacecraft applications can be considered well-known. Measurement and control of absolute attitude is a feature of practically every spacecraft. Onboard measurement of absolute position is required, e.g., in Earth observation missions, where receivers for satellite navigation and for ground-based radio-positioning systems, e.g. DORIS (Carrou 1995), are accommodated on the spacecraft. In most other missions, absolute orbit and position determination is usually done by observations from ground, since, in the majority of cases, mission requirements do not justify the accommodation of an absolute position sensor aboard the spacecraft.

The above-mentioned exception, to be described in this chapter, comprises the basic functional principles of absolute position measurement by satellite navigation. At the time of writing, GPS and GLONASS are the satellite navigation services used, and, for the purpose of rendezvous navigation, the navigation results of, e.g., GPS receivers w.r.t. an Earth-fixed coordinate frame, are termed *absolute GPS*. The understanding of absolute GPS is a pre-requisite for the understanding of *relative GPS*, which is one of the major sensor principles used nowadays for far and medium range relative navigation in the rendezvous approach. If a GPS receiver is available on board, absolute GPS will of course also be the main source of absolute position information.

It is not intended to describe in this chapter the details of actual sensor design implementations. The detailed design depends to a large extent on the availability of particular technologies at the time of development, which have been changing relatively quickly in the last decades. Also, for the comprehension of the typical function and performance of a particular sensor concept in the context of a rendezvous system, it is not absolutely necessary to have detailed knowledge of the actual design implementation. The purpose of this chapter is rather:

- to address briefly the requirements for the sensors in terms of parameters to be measured, the measurement performances in relation to trajectory errors and in relation to ranges of operation in the approach;
- to give a short overview of the physics which can be used for relative navigation measurements between two vehicles;
- to identify the basic functional principles of various categories of sensors actually used for rendezvous purposes;
- to discuss the potential disturbance effects which may result from the measurement environment for the various sensor principles;
- to identify typical features of the various sensor categories in terms of measurement performance, range, mass and power consumption and other constraints.

## 7.1 Basic measurement requirements and concepts

### 7.1.1 Measurement requirements

Measurements of the absolute state, such as the attitude of the vehicle w.r.t. the local orbital frame $\boldsymbol{F}_{\mathrm{lo}}$ and as position or orbital ephemerides of the vehicle in the Earth-centred equatorial frame $\boldsymbol{F}_{\mathrm{eq}}$, will be required during all phases of the rendezvous mission to determine spacecraft angles and position w.r.t. the Earth and the Sun for communication, power and illumination reasons. In addition, starting from the far range rendezvous, relative position and velocities need to be available in the target local orbital frame $\boldsymbol{F}_{\mathrm{lo}}$. Relative position and velocity information could of course be obtained by the differences of the absolute measurements made on chaser and target. However, as the subtraction of large values leads to large errors, this method can only be used at large distances. In the rendezvous phases proper, i.e. during far and close range rendezvous, an increasingly accurate knowledge of the relative position and velocities of the chaser w.r.t. the target is necessary. This requires direct measurements to be made between the two vehicles. Such measurements can in principle be performed on either vehicle. If performed on the target vehicle, the results would have to be transmitted to the chaser GNC system, which may cause additional noise and which includes the danger of link interruptions. If performed on the chaser, the vehicle's position or velocity cannot be measured directly in the target's $\boldsymbol{F}_{\mathrm{lo}}$ frame. In this case, the attitude of the sensor axes w.r.t. the $\boldsymbol{F}_{\mathrm{lo}}$ frame of the target must be known with sufficient accuracy in order to resolve the actual range and direction measurements made in the chaser body frame into the needed values w.r.t. the target local orbital frame.

### Measurement parameters

The following two alternatives can be used for the relative position measurements:

- Measurement of range and line-of-sight angles and of range-rate and angular velocities in the body frame $\boldsymbol{F}_{\mathbf{ge}}$ of chaser or target (for definition of frames see section 3.1). These measurements can be resolved into $x$-, $y$-, $z$-position and velocities in the $\boldsymbol{F}_{\mathbf{lo}}$ frame of the target, provided the attitude of the chaser in the target frame is known. The angular difference between the nominal attitude frames of chaser and target frame due to the curvature of the orbit can be calculated from the distance $r$ between the vehicles. At very small ranges ($r \ll R$, where $R =$ radius of orbit), the angular directions of chaser and target $\boldsymbol{F}_{\mathbf{lo}}$ frames are practically identical within the accuracy of attitude measurement and onboard calculation; e.g. below a range of 1 km the angular misalignment of the nominal frames of chaser and target is $<$0.009 deg.
- Measurement of range and/or range-rate on both chaser and target to a number of common external reference points, using the same type of tools and methods on both vehicles. The differential result will be calculated from the differences between the individual measurements on each vehicle, rather than taking the difference of the complete results. This is the type of measurement principle used, e.g., in RGPS, described in section 7.3.3. Because of the common reference points, tools and methods, and because the distance between chaser and target is small compared with the distance to the reference points, the major part of the errors will be the same on both chaser and target sides, and will therefore be cancelled during the subtraction of the measurements from both vehicles.

For the acquisition of the docking axis in the last part of the approach, control not only of the relative translational motion, but also of the angular motion between the docking frames of chaser and target is required. Therefore, additional information on relative attitude and relative attitude rate needs to be available. Again, the relative attitude between the two vehicles could in principle be obtained by calculating the difference between their absolute attitudes in the local orbital frame. However, because of the potential accumulation of errors, and because of the limitations of the reception range of the docking mechanism, it will, in most cases, be necessary to measure the relative attitude directly between the docking ports of the two vehicles. Deviations of the actual from the nominal relative attitude of the docking interfaces can be due to:

(1) potential unknown misalignments of the docking axes w.r.t. the nominal attitude frames on both vehicles, e.g. due to thermal expansion;

(2) motions of the docking axis, which are independent of motions of the vehicle's nominal attitude frame w.r.t. the $\boldsymbol{F}_{\mathbf{lo}}$ frame, e.g. due to structural flexibilities;

(3) instantaneous deviations from the nominal attitude due to the control motion (see figure 8.30),

The most important requirement for the rendezvous navigation is that the measurement errors for all parameters are decreasing commensurate with the decreasing range between the two vehicles. The second important requirement is that, in the vicinity of the docking port, the navigation errors become small enough to keep the control errors within the reception range of the docking mechanism (see section 8.3.6) or within the tolerances of the inner berthing box (see section 5.3.1). In order to arrive at the sensor requirements, the effects of measurement errors on the trajectory and the possibility of reducing the manoeuvre errors, or of achieving converging errors in the trajectory sequence by other means, will be discussed below.

**Position measurement errors**

Only position measurement errors in the $z$-direction (R-bar) have significant effects on the trajectory evolution. The lateral measurement error, $\Delta z_{\mathrm{m}}$, can translate, as has been discussed in section 4.3.1, into an error in the $x$-direction in two ways. First, case (a), if the chaser is on a concentric orbit with a different radius from the target orbit, an unobserved altitude difference of $\Delta z_{\mathrm{m}}$ results, according to Eq. (4.16),

- after one orbital revolution (tangential boost transfer) in a position error along the orbit direction of $\Delta x = 3\pi\Delta z_{\mathrm{m}}$,
- after half an orbital revolution (radial boost transfer) accordingly in $\Delta x = 3/2\pi\Delta z_{\mathrm{m}}$.

Secondly, case (b), if the chaser is actually above or below the target orbit, but has the same velocity in the orbit direction as the target, an unobserved altitude difference of $\Delta z_{\mathrm{m}}$ results, according to Eq. (4.17),

- after one orbital revolution (*T*) in a position error along the orbit direction $\Delta x = 12\pi\Delta z_{\mathrm{m}}$,
- after half an orbital revolution (*T*/2) in an $x$-position error of $\Delta x = 6\pi\Delta z_{\mathrm{m}}$ and a $z$-position error of $\Delta z = 7\Delta z_{\mathrm{m}}$.

The numeric values given in section 4.3.1 are repeated here for reference. For a measurement error of $\Delta z = 10$ m, the results would be:

case (a) at *T*/2, $\Delta x = 47.12$ m; at $T$, $\Delta x = 94.25$ m

case (b) at *T*/2, $\Delta x = 188.5$ m, $\Delta z = 70$ m; at $T$, $\Delta x = 377$ m, $\Delta z = 0$

Whether measurement error case (a) or (b) is applicable could be decided only if very accurate velocity measurements were available. Since the accuracy of velocity measurement is, in most cases, worse than that of the position measurement, case (b) has to be taken into account as the worst case for the position error at arrival.

### Velocity measurement errors

In addition to the position measurement errors, the dispersion of the final position is also sensitive to errors in the velocity measurement, as has been shown in section 4.3.1. According to Eq. (4.18), a velocity measurement error $\Delta V_{x\mathrm{m}}$ in the orbit direction will cause

- after half an orbital revolution (radial boost transfer) a position error of $\Delta x = -\frac{3}{2}\Delta V_{x\mathrm{m}}T$ and $\Delta z = -\frac{4}{\omega}\Delta V_{x\mathrm{m}}$,
- after one orbital revolution, a zero position error in the $z$-direction, and a position error in the $x$-direction of $\Delta x = -3\Delta V_{x\mathrm{m}}T$.

The numeric values given in section 4.3.1 are repeated here for reference. A velocity measurement error in the orbit direction of only 0.01 m/s would, after one orbital revolution, lead to an $x$-position error of about 170 m with no $z$-position error, and after half a revolution to an $x$-position error of about 85 m and a $z$-position error of about 36 m.

The effect of velocity measurement errors in the $z$-direction, $\Delta V_{\mathrm{zm}}$, is much smaller than that of $\Delta V_{\mathrm{xm}}$ errors, i.e. 0.21 times ($= \frac{2}{3\pi}$) on the $x$-position, and 0.25 times on the $z$-position (see Eq. (3.34)). Velocity measurement errors in the $y$-direction, $\Delta V_{y\mathrm{m}}$, result in position errors only in the $y$-direction. The effect of $\Delta V_{y\mathrm{m}}$ on the the $y$-position is the same as that of $\Delta V_{\mathrm{zm}}$ on the the $z$-position.

As for the position error, the velocity measurement error must decrease linearly with the range, in order to remain within a particular final position error in relation to the range. Otherwise, it must have the performance for the shortest distance over the entire range of use.

### Angular measurement errors

For sensors which calculate position and velocities from line-of-sight (LOS) angles and range, the LOS measurement accuracy needs to be compatible with the range measurement accuracy. The lateral error is $\Delta z = r \cdot \sin \Delta\alpha$, where $\Delta\alpha$ is the LOS angle measurement error. The angular accuracy must be, therefore, at least 0.05 deg in order to correspond to the 0.1% of range requirement. Considering that errors in both range and LOS angle measurement will occur, the individual contributions must be accordingly lower.

Effects of measurement errors on absolute attitude are not considered here, as absolute attitude is not measured by rendezvous sensors. Relative attitude needs to be measured only in the last phase of approach on closed loop controlled straight line trajectories. Relative attitude errors will be addressed below in the context of capture conditions.

### Effects on trajectory strategy and safety

From the above considerations, it is obvious that, with open loop transfers, a constant measurement accuracy for the lateral position will not be sufficient to achieve final contact conditions. However, if the measurement accuracy is a certain percentage of the range, i.e. if the errors decrease steadily with the distance to the target, larger measurement errors can, to a certain extent, be compensated for in the approach strategy by more and shorter steps at the expense of a longer duration and higher propellant consumption.

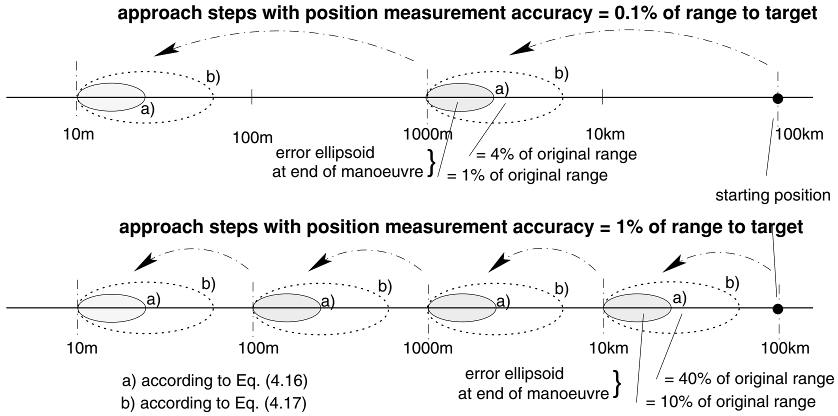


Figure 7.1. Approach steps with 0.1% and 1% of the range sensor accuracy.

*Example 1*

In figure 7.1, tangential boost transfers along the orbital axis are assumed, i.e. each transfer takes one orbital revolution. Two sensors are considered: the first has a measurement accuracy for lateral position of 0.1% of the range to the target, and the second has a position measurement accuracy of 1% of the range. Let us look at the transfer from a range of about 100 km to a range of 1000 m from a target station.

For a sensor with a lateral measurement error of 0.1% of the range, the range error would at arrival be approximately 1% of the original range, i.e. 1000 m for measurement error case (a) and about 4%, or 4000 m, for measurement error case (b).

In the second case, with a lateral measurement error of 1%, the range error at arrival would be 10% of the original range, i.e. 10 km for measurement error case (a) and about 40%, or 40 km, for measurement error case (b).

In the case of a 1% lateral measurement accuracy, the targeted position for a transfer in the $x$-direction must be no closer than 40 km for lateral measurement error case (b), in order to avoid the danger of collision with the target. As a result, the transfer from 100 km to 1 km must be performed with this sensor performance in at least two steps, whereas for a sensor of 0.1% accuracy, the same absolute final dispersion could be achieved in one step.

This example shows that, as a result of the measurement accuracy of the sensor, there is a limit to the size of the manoeuvres. By introducing a larger number of manoeuvre steps of shorter transfer distance, using a lower performance sensor, the final accuracy can still be achieved. In any case, the error ellipsoid around the arrival position must be at sufficient distance from the target vehicle, so that there will be a limit to the acceptable sensor errors.

Whereas for tangential boost transfers, lateral measurement errors result, after one orbital revolution, in position errors only along the $x$-direction (V-bar), in the case of radial boost transfers, the position error after half an orbital revolution will also include, as we have seen, significant components in the $z$-direction. This will make the correction of position errors after each transfer step more complex, as corrective $\Delta V$s in the tangential and radial directions will be required. Dispersions due to measurement errors in the $z$-position and the $x$-velocity are shown in figure 7.2. Combinations of position and velocity measurement errors can also lead to problems in the assessment of trajectory safety, which can be demonstrated by the following example.

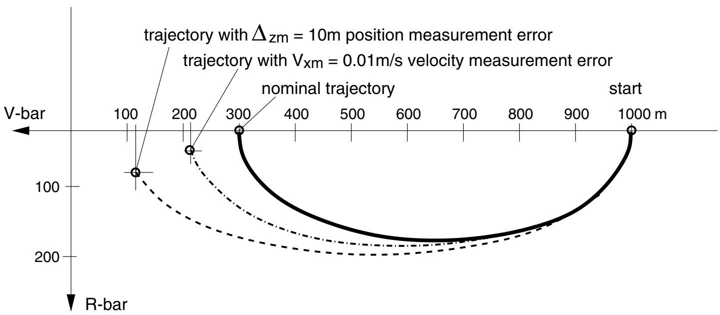


Figure 7.2. Dispersions due to measurement errors after radial boost transfer.

*Example 2*

Let us consider a radial boost manoeuvre along V-bar from a starting distance of 1000 m to an end distance of 300 m from the target: the $z$-position measurement error is $-10$ m and the $x$-velocity error is $-0.006$ m/s. Assuming that in reality the chaser is 10 m below V-bar and at zero relative velocity w.r.t. the target, the sensor would in this case indicate a position on the target orbit and a relative velocity of $-0.006$ m/s, i.e. a safe condition for a $-$V-bar approach. With the actual initial conditions, after half an orbital revolution the position error would be of the order of 190 m in the $x$-direction and 70 m in the $z$-direction.

The example shows that for an open loop radial boost transfer, starting at 1000 m and targeted at a few hundred metres, the assumed measurement accuracies of 1% of range and 0.006 m/s would lead to unacceptable end conditions for the transfer.

### Velocity measurement by differentiation

In many cases the velocity cannot be measured directly or cannot be measured with the required accuracy. If a sensor can only measure the position, the average velocity can be obtained from the change of position over time. If, e.g., its position measurement accuracy were 10 m, an undisturbed measurement duration of 1667 s would be necessary to obtain a resolution of 0.006 m/s, i.e. the velocity measurement accuracy assumed in example 2 for a manoeuvre initiation at 1000 m. The measurement time will of course be shorter if velocities can be measured directly. With a direct velocity measurement capability of 0.1 m/s (the approach velocities are of the order of 10 m/s prior to the manoeuvre to acquire the target orbit, and 1–2 m/s during closing), it would take a measurement duration of only 16.7 s to reach the same resolution. However, the requirement to reduce position and velocity measurement errors commensurate with the decreasing distance to the target will, at close range for open loop transfers, eventually lead to unfeasible measurement requirements, both for accuracy and duration, and will rule out, for trajectory safety reasons, open loop transfers below a certain range to the target.

### Mid-course corrections and closed loop control

The position accuracy of impulsive transfer manoeuvres can be improved by one or more intermediate corrections (mid-course corrections) or by closed loop control of the nominal trajectory, calculated for the nominal boosts (see section 4.4.1). In the case of a single mid-course correction manoeuvre, the final position errors can be reduced theoretically to one-half, by a further correction manoeuvre at three- quarters of the orbital revolution to one-quarter of the original value. As each manoeuvre will introduce new errors, this theoretical improvement may not be achievable in reality.

In the case of closed loop control over the entire transfer trajectory, the error at arrival will be the measurement error plus some additional control error. It is the major advantage of continuous closed loop control that the effects of initial measurement errors will be controlled out. This is due to the fact that, in closed loop trajectories, the position errors are a function of the range of the actual trajectory point, rather than of the range at manoeuvre initiation from the target, as in open loop transfers. As a result, for continuously controlled two-boost transfer trajectories, the requirements for position and velocity measurement in all directions will be less tight than in the case of the open loop transfers.

For closed loop trajectories the measurement accuracy should be, where possible, an order of magnitude (but as a minimum two to three times) better than that of the value to be controlled. For reasons already discussed above, the last part of the approach needs to be a straight line transfer. During the straight line final approach, not only the position, but also the velocity profile needs to be controlled accurately; this leads to additional velocity measurement requirements.

**Measurement requirements at capture**

The most critical measurement and control requirements must eventually be met at capture. The limiting features at capture are:

- in docking, the useful reception range of the docking mechanism in terms of lateral and angular misalignments and impact velocities (see section 8.3);
- in berthing the location and size of the inner berthing box (see section 5.3.1).

The following parameters are to be controlled, and performances are to be achieved, by the GNC system, for the interface with the capture operations.

- *For docking:* approach velocity, lateral alignment, lateral velocity, angular alignment and angular rate. Depending on the type of docking mechanism and vehicle characteristics, the typical values for docking are:

  approach velocity = 0.03–0.3 m/s

  lateral alignment = 0.05–0.2 m

  lateral velocity = 0.01–0.05 m/s

  angular misalignment = 1–5 deg

  angular rate = 0.05–0.25 deg/s

- *For berthing:* the nominal velocities at inhibit of actuation must be zero. The typical performance values to be achieved in the berthing box are:

  $x$-, $y$-, $z$-position = 0.1–0.5 m

  residual velocities = $<$ 0.01 m/s

  angular misalignment $\leq$ 10 deg

  angular rate: $\leq$ 0.1 deg/s

Because of the time required for the capture process to take place, the linear and angular rates are, in the case of berthing, more critical than the initial linear and angular misalignments.

It has been discussed in chapter 4 that navigation errors are not the only source of trajectory deviations and misalignments at capture. They will form, therefore, only a part of the overall error budget. In figure 7.3 an example of an allocation of error sources is shown for the closed loop controlled final translation to docking as a pie-chart. The main contributors to the final alignment accuracy at contact are:

- the sensor measurement error, including the sensor noise and any uncompensated bias resulting from the sensor itself and from misalignment between the sensor and the docking axis;

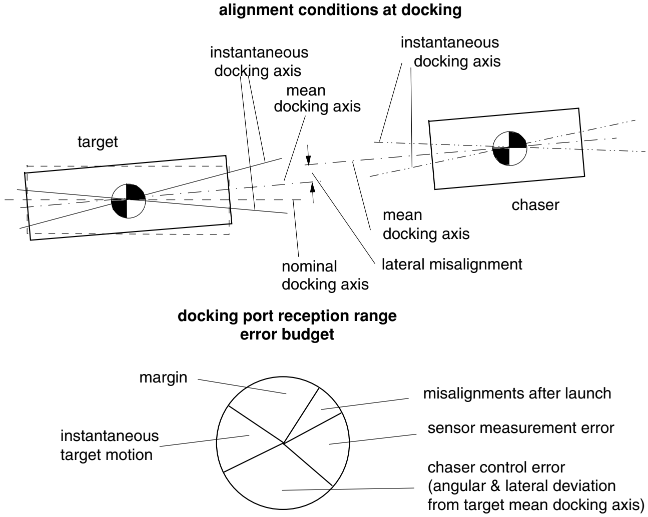


Figure 7.3. Error allocation for docking reception range.

- the control error, including all deviations of the actual vehicle state w.r.t the one according to the guidance set values and state as measured by the sensor;
- the uncompensated misalignments between the sensor axis and the chaser docking axis and between the target reflector axis and the target docking axis, e.g. due to residual calibration errors, launch impact and thermal deformations;
- the motion of the target which cannot be detected by the sensor, e.g. because of limited sensor bandwidth;
- a margin which covers all other unknown deviations and disturbances.

### Conclusions on measurement performance

From the above discussion, the following conclusions on the effects of the performance of sensors for relative navigation can be drawn.

**Impulsive transfers** In open loop:

- The most significant trajectory deviations are caused by measurement errors of position in the $z$-direction (R-bar) and of velocity in the $x$-direction (V-bar).
- For open loop transfers, the end position of the transfer must be sufficiently far from the target such that the position dispersions at the end of the transfer do not lead to collision danger. The initial accuracy of position knowledge (all axes) should be

0.1% of range or better. An accuracy of only 1% may lead in two-pulse transfers to final position dispersions, which are unacceptable in the medium and short range rendezvous phases.

- Open loop transfer accuracy can be improved by mid-course corrections, taking advantage of the increased measurement accuracy at reduced distance to the target. In addition to a reduced transfer distance, one or more intermediate corrections will be necessary to make an approach with a 1% of range measurement accuracy viable down to ranges to the target of one or two kilometres. For an approach with mid-course corrections down to a few hundred metres, lateral position measurement accuracy would have to be at least 0.1% of range.

- If the lateral position is derived from range and LOS measurements, a range measurement accuracy of half the lateral measurement accuracy must be achieved as a minimum.

- LOS angles need to be measured with an accuracy of $\leq$0.25 deg, if, together with the range error of 0.5%, a lateral position measurement error of $<$1% of range shall be kept and accordingly a factor of 10 better, if a position measurement error of 0.1% has to be achieved.

- A 0.01 m/s velocity measurement error in the orbit direction will cause, in an impulsive, transfer a position error in the $x$-direction of about 85 m after half an orbital revolution and about 170 m after one revolution and a $z$-error of about 36 m after half a revolution. Errors of this size will not be acceptable at ranges to target below one or two kilometres. For an approach down to a few hundred metres to the target, the velocity measurement performance would have to be an order of magnitude better.

To achieve the required velocity measurement accuracy from position measurements, a long integration time may be necessary.

In closed loop:

- In impulsive transfers there is a possibility of reducing the dispersion at the arrival position by employing closed loop control w.r.t. a nominal trajectory. As measurement errors are a function of the range of the actual trajectory point, a 1% of range sensor accuracy, together with other error contributors, in a closed loop controlled transfer, may permit position accuracy of a few per cent of the actual range.

- For the closed loop controlled two-pulse transfers, the initial velocity measurement accuracy will be less critical, if along the trajectory the position measurement accuracy at each point is sufficiently accurate. A continuous position control with a measurement accuracy of 1% of range will provide sufficient integration over the transfer duration for effective correction of initial velocity errors.

### Straight line transfers

- For closed controlled trajectories terminating with capture, it has to be kept in mind that the final position accuracy is determined also by other errors, as shown in figure 7.3. Measurement errors must be a factor of 2–5 lower than the desired final accuracy.
- For closed loop controlled trajectories with a velocity profile, the velocity measurement accuracy should be, if possible, one order of magnitude (but at least a factor of 2) better than the desired velocity accuracy. If, e.g., the nominal velocity of the last metre approach to contact were 0.1 m/s, and was to be controlled with 20% accuracy, the velocity measurement accuracy must be $<1$ cm/s.
- To achieve such velocity accuracy by position measurement, range and LOS angles must be measured with a bandwidth of the order of 1 Hz or better. Additional requirements for the bandwidth of the sensor can be imposed in the short range by the motion of the target, e.g. due to attitude control motions or structural oscillations. Lateral motion of the target which cannot be followed by the chaser is a major contributor to the error budget for docking.
- The measurement accuracy for relative attitude must be about 1 deg, if an angular alignment of the docking axes of $<5$ deg is to be achieved.

The above discussion was intended to show the driving factors for sensor requirements; it was not intended to yield a complete list of specifications for rendezvous sensors. Such specifications can be derived only after the definition of an approach strategy, including trajectory types and transfer distances, after decisions on mid-course correction schemes and closed loop control of trajectories, and after proper analysis of the other sources of trajectory deviations, such as external disturbances and thrust errors.

## 7.1.2 Measurement principles

The following basic physical phenomena and principles can be exploited for the measurement of the navigation parameters required during the rendezvous process.

### Distance, range

- Triangulation. The range is calculated from measured angles and known target dimensions: measurement on the chaser of the direction angles toward a number of reference points on the target or vice versa (the relative position of those reference points w.r.t. each other must be known); measurement of the size of an image of a feature on the target in the focal plane of a camera on the chaser or vice versa (the dimensions of the feature must be known).
- Time of flight from a transmitter to a receiver of an electro-magnetic wave signal. This requires knowledge of the time $t_0$ when the signal is radiated (see figure 7.5).

- Phase shift of an electro-magnetic wave signal at a receiver w.r.t. the phase at the transmitter. This requires the knowledge of the phase when radiated (see figure 7.5).
- Integration over time of a velocity measurement. This will only provide the *changes* in range over the measurement period, not the absolute range.

**Range-rate**

- Doppler shift of transmitted frequency, when arriving at receiver (see figure 7.7). This requires the knowledge of the transmitter frequency.
- Differentiation w.r.t. time of range measurements. This requires a sufficiently low noise factor in the range measurements.

**Line-of-sight direction**

- Measurement of the position of a target point or of the centre of a target image in the focal plane of a camera (see figures 7.30 and 7.31).
- Difference of phase delay measurement by two antennas, mounted at a fixed distance on one of the vehicles, of an electro-magnetic wave transmitted or reflected by a target on the other vehicle (see figure 7.10).
- Difference of time delay measurement by two antennas, mounted at a fixed distance on one of the vehicles, of an electro-magnetic wave transmitted or reflected by a target on the other vehicle (see figure 7.10).
- Measurement of the signal transmitted or reflected by the other spacecraft concerning signal amplitude and instantaneous angle of the rotating receiver antenna at reception. The antenna must have a suitable pattern, with a pronounced maximum or minimum strength (see figures 7.11 and 7.12).
- Measurement of gimbal angle, or of electronic scan angle, at reception of a narrow beam signal, either transmitted or reflected by the other spacecraft (scanner type, see figure 7.9).

**Relative attitude**

- Triangulation. A three-axes frame on the target is established by: measurement of range and direction of at least three different known points, forming a plane (see figure 7.29); relative position of target image in the focal plane of a camera of at least four known target points forming a three-dimensional body (see figure 7.31).

- Single-axis measurement by superposition of two antenna patterns, i.e. by a fixed antenna with tone modulation and by a rotating antenna: an omni-directional antenna transmits a tone modulated signal, a second antenna with a particular antenna characteristic rotates with the modulation frequency, measurement of phase difference between the two-tone signals; this is similar to a VHF omni-directional range (VOR) in aircraft navigation (see figure 7.13).

- Single-axis measurement by two, and two-axis measurement by four, antenna beams with different modulation frequencies, measurement of amplitude difference (similar to instrument landing system (ILS) in aircraft navigation (see figure 7.14).

**Angular rate**

- Differentiation w.r.t. time of LOS and relative attitude measurements.

- Gyroscopes. Gyroscopic effects (mechanical: conservation of angular momentum; optical: Sagnac effect) are the only physical phenomena available for direct angular rate detection. Gyroscopes cover, however, only the angular motion of their own vehicle w.r.t. the inertial frame. They do not measure, e.g., the rate of LOS due to lateral motions of the target or the rate of relative attitude due to attitude changes of the target.

# 7.2 RF-sensors

## 7.2.1 Principles of range and range-rate measurement

### General principle of range measurement

The range of the target can be measured either by measurement of the time of flight of the signal or by measurement of the phase shift of the incoming w.r.t. the outgoing signal. This requires recording in the first case the time and in the second case the phase both at transmission and reception. The relationship between the time-of-flight, $t_2 - t_1$, of an electro-magnetic wave and the travelled distance, $r$, is given by the speed of light $c$:

$$t_2 - t_1 = \frac{r}{c} \tag{7.1}$$

and the relationship between the shift of phase, $\phi_2 - \phi_1$, and the travelled distance, $r$, is

$$\phi_2 - \phi_1 = \frac{2\pi r}{\lambda} = \frac{2\pi r f}{c} \tag{7.2}$$

where $\lambda$ is the wavelength and $f$ is the frequency of the signal. In the general case these time or phase differences can be measured only when the transmitted signal is reflected by the target and the reflected signal is received again at the location of the transmitter (for an exception see section 7.3.2). In all practical cases, a modulated RF signal is generated by a transmitter and is transmitted by an antenna toward a target. Part of the power of the signal is reflected by the target back in the direction of the transmitter, or the signal is re-transmitted by a transponder on the target, and is received by an antenna at the transmitter location. Transmitting and receiving antenna may be the same piece of hardware if there is a switching function between outgoing and incoming signal. Because of the modulation, the returning signal (echo) can be referenced to the outgoing signal.

### Range measurement with pulse modulated signal

A high frequency carrier is modulated in pulse form. The time of the flank of the received pulse is related to that of the transmitted one. The total time will be double the amount given by Eq. (7.1), as the range $R$ has to be travelled twice by the signal:

$$T = \frac{2R}{c}$$

Hence the range is

$$R = \frac{1}{2} T \cdot c \tag{7.3}$$

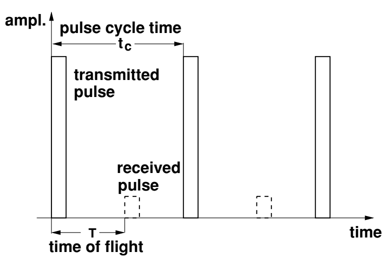


Figure 7.4. Functional principle of range measurement via time delay.

In order to avoid interference between the transmitted and received signals, in pulse radars, where the same pulse is repeatedly sent out, the subsequent pulse can only be sent after the echo of the previous one has been received. The receiver has to be blocked while a pulse is transmitted. This is true for the basic measurement principle of pulse type radars. In more modern developments the pulse is not created by switching the carrier frequency on and off, but by bi-phase modulation (see below). For a resolution of 1 m, the system must be able to measure a time difference of $\leq 6.6 \times 10^{-9}$ s.

### Range measurement with continuous wave signal

Measurement of the phase difference between transmitted and received signals requires the knowledge of the phase at transmission. As in the time-of-flight measurement above, the initial conditions at transmission are available, in general, to a receiver, if it is collocated with the transmitter and if the signal is reflected by a target. This measurement principle is used by CW-type radars and also generally used by ground stations of satellites for so-called 'tone ranging' via two-way telemetry links. A continuous wave signal is transmitted toward the target. The phase difference between the transmitted and the echo signals is

$$\Phi = 2\frac{2\pi R}{\lambda} \tag{7.4}$$

where $\lambda = \frac{c}{f}$ is the wavelength. The range is then accordingly:

$$R = \frac{\Phi\lambda}{4\pi} \tag{7.5}$$

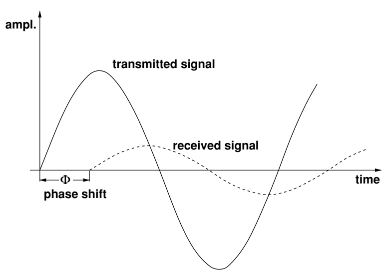


Figure 7.5. Functional principle of range measurement via phase shift.

As $\Phi$ can be measured unambiguously only between 0 and $2\pi$, the measurements become ambiguous at ranges of $2R > \lambda$. On the other hand, the resolution of the range measurement increases when the wavelength decreases. If e.g. the frequency used for the measurement is 10 kHz, the maximum range which can be measured unambiguously

$$R = \frac{1}{2}\lambda = 15 \text{ km}$$

and if the phase angle can be measured with an accuracy of $\Delta\Phi = 0.01$ rad, the resolution will not be better than

$$\Delta R = \frac{1}{2}\frac{\lambda}{2\pi} = 24 \text{ m}$$

To improve the range, the wavelength would have to be increased, but to improve the resolution, it would have to be decreased. A solution to this dilemma is the use of two or more modulation frequencies, where the highest frequency determines the resolution and the lower ones determine the wave range (Hartl 1977). One possibility would be to modulate different subcarrier frequencies on the main carrier, which could again be modulated to transmit additional information.

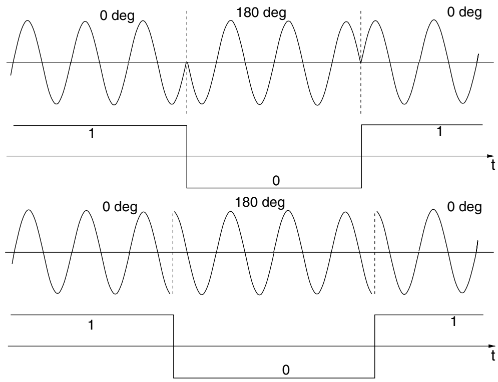


Figure 7.6. Bi-phase modulation of carrier frequency.

A method often used for such modulation is a phase modulation with the phase angles $\Phi$ equal to 0 and 180 deg, often called 'phase shift key' (PSK). This type of modulation, which can be used to transmit pulse type or digital information, is shown in figure 7.6. A logical '0' or a logical '1' corresponds in this case to one of the two phase angles. In radar applications, pulses of different length or a code of '0s' and '1s' can be used to indicate the start of the time measurement on the signal. Phase angle measurement according to Eq. (7.5) can be performed on the main and subcarriers, and time-of-flight measurement according to Eq. (7.3) on the digital code. Such a combination of pulse and phase radar principles is used in the Kurs system and in the satellite navigation systems described in sections 7.2.5 and 7.3.

### Range-rate measurement

For the measurement of the range-rate, use can be made of the Doppler effect. The 'Doppler shift' of a frequency arriving at a receiver is directly proportional to the component of the relative velocity, $\dot{R}$, in the transmitter–receiver direction:

$$\Delta f = \frac{-\dot{R} f_{\mathrm{T}}}{c} \tag{7.6}$$

i.e. when the range-rate is positive, which means that the transmitter moves away from the receiver and the range increases with time, the frequency $f_{\mathrm{R}}$ arriving at the receiver becomes lower; and vice versa, when the range decreases with time:

$$f_{\mathrm{R}} = f_{\mathrm{T}} + \Delta f = f_{\mathrm{T}}\left(1 - \frac{\dot{R}}{c}\right) \qquad (7.7)$$

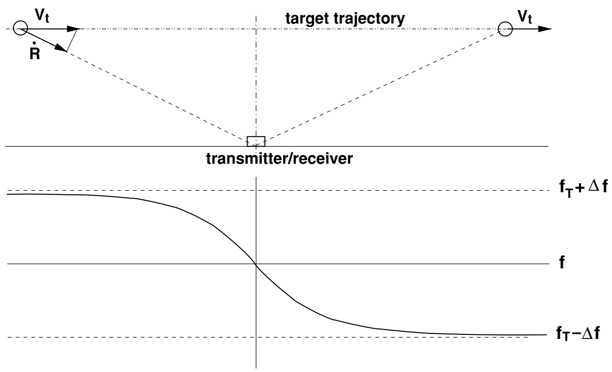


Figure 7.7. Doppler shift of received frequency due to target range-rate.

If the signal is reflected at a target, the Doppler shift will be applied twice. The frequency at the target is

$$f_{\mathrm{t}} = f_{\mathrm{T}}\left(1 - \frac{\dot{R}}{c}\right)$$

and the frequency at the receiver is

$$f_{\mathrm{R}} = f_{\mathrm{t}}\left(1 - \frac{\dot{R}}{c}\right)$$

resulting in

$$f_{\mathrm{R}} = f_{\mathrm{T}}\left(1 - \frac{\dot{R}}{c}\right)^2 \qquad (7.8)$$

which, since the velocity of light, $c \gg \dot{R}$, is, to a good approximation,

$$f_{\mathrm{R}} = f_{\mathrm{T}}\left(1 - 2\frac{\dot{R}}{c}\right) \qquad (7.9)$$

The range-rate is then

$$\dot{R} = \frac{1}{2}\frac{c}{f_\mathrm{T}}(f_\mathrm{T} - f_\mathrm{R}) \tag{7.10}$$

or

$$\dot{R} = \frac{1}{2}\lambda_\mathrm{T}(f_\mathrm{T} - f_\mathrm{R}) \tag{7.11}$$

where $\lambda_\mathrm{T}$ is the wavelength of the transmitted signal.

This measurement principle is used by Doppler radars. In order to obtain a velocity resolution of 0.01 m/s, such a sensor must be able to measure a ratio of $\frac{\Delta f}{f} = 6.7 \times 10^{-11}$, which requires transmission frequencies of the order of 100 GHz.

### Power limitations of operating range

The maximum range of a radar is limited by the lowest power of the returning signal which can be detected on the receiver side. This means that the received signal must be at a sufficiently high level above the noise. Noise may be created both by external sources or by the receiver itself. Thermal noise will eventually form the limit for the receiver sensitivity. The power density of the signal when arriving at the target is equal to the transmitted power times the ratio of the transmitter antenna gain to the surface of a sphere with the radius of the range *R*:

$$S_\mathrm{t} = \frac{P_\mathrm{T} G_\mathrm{T}}{4\pi R^2} \tag{7.12}$$

where $S_\mathrm{t}$ is the power density of the signal at target, $P_\mathrm{T}$ is the power of the transmitted signal and $G_\mathrm{T}$ is the power gain of the transmitting antenna. The power reflected by the target is equal to the power density at the target times the effective reflecting area of the target. Assuming diffuse, i.e. omni-directional, reflection by the target, the power density of the echo signal when arriving at the receiver is

$$S_\mathrm{echo} = \frac{S_\mathrm{t} A_\mathrm{te}}{4\pi R^2} \tag{7.13}$$

where $S_\mathrm{echo}$ is the power density at the receiver antenna, $A_\mathrm{te}$ is the effective area of the target, resulting in the well-known 'radar equation' (Ehling 1967):

$$S_\mathrm{echo} = \frac{P_\mathrm{T} G_\mathrm{T} A_\mathrm{te}}{(4\pi R^2)^2} \tag{7.14}$$

Multiplying this result by the effective area $A_\mathrm{re}$ of the receiver antenna yields the received power:

$$P_\mathrm{rec} = S_\mathrm{echo} A_\mathrm{re} \tag{7.15}$$

These signal power considerations apply to all radar types with passive reflection.

### Transponder on target

As the power of the echo is inversely proportional to the fourth power of the range, there will eventually be a limitation in the operational range, outside of which such a system cannot be used: for the long range by the signal-to-noise ratio and for the short range by saturation of the amplifiers. A passive measure taken to improve the power of the return signal is the placing of a corner-cube reflector on the target. A method used to increase significantly the power density of the return signal consists of placing a transponder on the target; this amplifies the received signal and re-transmits it toward the transmitter using a directional antenna and a different frequency. This has the additional advantages that a de-coupling of transmitted and received signals is achieved, and that no switching between transmit and receive mode is necessary. The time delay of the signal on its way through the transponder must of course be known and must be constant over time.

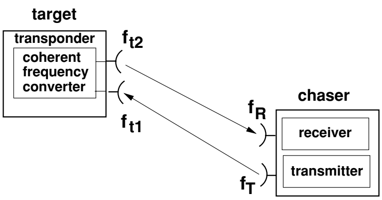


Figure 7.8. Frequency conversion and re-transmission by transponder.

For range measurement in Eq. (7.3), the transponder delay time $t_\mathrm{t}$ has to be added to the time-of-flight $T$, i.e. $T_\mathrm{tot} = T + t_\mathrm{t}$. In the same way, the phase delay of the transponder, $\phi_\mathrm{t} = 2\pi f \cdot t_\mathrm{t}$, has to be added to the phase shift $\Phi$ in Eq. (7.5), i.e. $\Phi_\mathrm{tot} = \Phi + \phi_\mathrm{t}$.

In a Doppler radar the frequency transmitted by the transponder must have a fixed relation to the received frequency, e.g. by a factor $n$, in order to take into account the Doppler shift correctly on both legs:

$$\frac{f_\mathrm{t1}}{f_\mathrm{t2}} = n$$

The frequency at the receiver is then

$$f_\mathrm{R} = n f_\mathrm{T} \left(1 - \frac{\dot{R}}{C}\right)^2 \tag{7.16}$$

which is, as seen before to a good approximation,

$$f_\mathrm{R} = n f_\mathrm{T} \left(1 - 2\frac{\dot{R}}{c}\right) \tag{7.17}$$

The range-rate is then

$$\dot{R} = \frac{1}{2}\lambda_{\mathrm{T}}\left(\frac{1}{n}f_{\mathrm{R}} - f_{\mathrm{T}}\right) \tag{7.18}$$

### 7.2.2 Principles of direction and relative attitude measurement

Many of the measurement principles for direction and relative attitude measurements used in RF-sensors and described hereafter can be found in the literature on aircraft navigation systems, such as Kendal (1987) and Jenkins (1991).

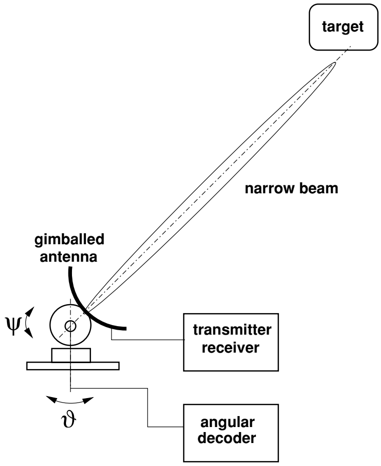


Figure 7.9. LOS measurement by pointing of narrow beam toward target.

#### Measurement of line-of-sight direction

**Pointing of narrow beam antenna** The most straightforward way of LOS direction measurement is the pointing of a narrow beam antenna toward the target. The transmitting/receiving antenna is mounted on a two-axis gimbal system, and the gimbal angles are measured for the maximum amplitude of the return signal. This maximum is usually found by scanning around the expected direction of the target. Since the time-of-flight of the reflected signal is very much smaller than a scan cycle, the gimbal angles at transmission and reception are identical within the accuracy of the angular read-out device. Electro-magnetic resolvers, optical encoders or similar devices can be used as read-out devices. This principle of LOS angle measurement by means of a scanning antenna is known from radar types of sensors, where range is measured according to Eqs. (7.3) or (7.5) and possibly range-rate according to Eqs. (7.10) or (7.11).

Instead of a gimbal system, which moves the entire antenna dish, scanning can be achieved also e.g. by angular motion of the antenna feeder or by electro-magnetic deflection of the antenna beam (electronic scanning). Where the achievable scan angle is sufficient, these methods will be preferred, because of reduced size and mass of the the assembly.

**LOS measurement via time delay or phase shift** In this type of sensor the time delay or phase shift is measured between a signal received by two antennas mounted on a baseline at a distance $d$. If the wave front is parallel to that baseline, both antennas receive the signal with the same phase. If the wave front is in line with the baseline, the phase shift and time delay will be according to their distance $d$. The signal arriving at antenna 1 (see figure 7.10) is

$$a_1(t) = a \cdot \sin(\omega t)$$

and at antenna 2 with the phase shift $\tau$:

$$a_2(t) = a \cdot \sin(\omega t + \tau) \tag{7.19}$$

or with the time delay $\Delta t$:

$$a_2(t) = a \cdot \sin[\omega(t + \Delta t)] \tag{7.20}$$

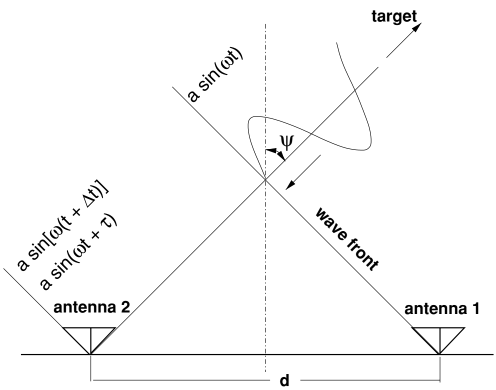


Figure 7.10. Functional principle of LOS measurement via two antennas.

The angle $\phi$ between the line toward the signal source and the line perpendicular to the baseline can be derived from the phase shift,

$$\tau = \frac{2\pi d}{\lambda} \sin\psi \tag{7.21}$$

or the time delay,

$$\Delta t = \frac{d}{c} \cos \psi \tag{7.22}$$

The resolution of the LOS angle $\phi$ will improve with increasing length of the baseline $d$ and with increasing resolution of the measurements of the time delay $\Delta t$ and the phase shift $\tau$. In the latter case the resolution will actually improve with a decrease of the wavelength $\lambda$.

**LOS measurement via amplitude and antenna rotation angle** The antenna characteristic of a dipole has two pronounced directions with zero reception (see figure 7.11), which can be used for direction finding. This will provide ambiguous results when bearing angles up to 360 deg have to be measured. However, in many applications it is known in which part of the circle the target has to be searched, so that this ambiguity does not play a role. The induced voltage over the rotation angle in a dipole antenna is

$$V(\phi) = V_{\max} \sin \psi \tag{7.23}$$

If the direction angle needs to be measured in the full range of 360 deg, the dipole characteristic can be superimposed on to a circular antenna pattern with the same sensitivity. The resulting antenna pattern is that of a cardioid (figure 7.12), which has one zero point. The combined induced voltage over the rotation angle in this arrangement is

$$V(\phi) = V_{\max}(1 + \sin \psi) \tag{7.24}$$

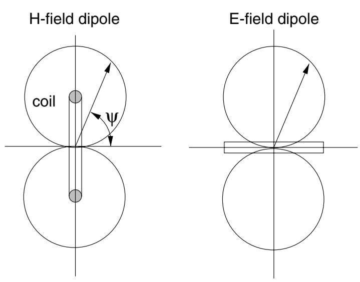


Figure 7.11. Antenna characteristic of dipoles.

## Measurement of relative attitude

**Relative attitude measurement through tone modulation and rotating pattern on target** On the transmitter side, an antenna (1) with a defined single maximum or minimum over the circumference, e.g. a cardioid characteristic, is rotated with a frequency

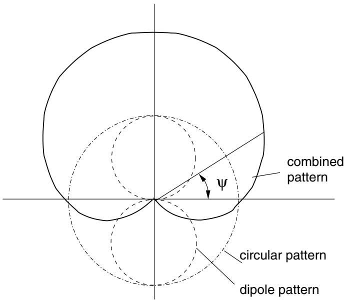


Figure 7.12. Cardioid antenna pattern.

of $n$ hertz. The antenna transmits a carrier signal without modulation. The signal received at a receiver antenna will be amplitude modulated with the rotation frequency $n$ of the transmitter antenna. A second antenna (2) on the transmitter side with a circular characteristic transmits a tone modulated signal with the frequency $n$. Rotation of antenna (1) and amplitude modulation of antenna (2) are adjusted in such a way that, in a particular direction, a receiver will receive both signals without phase difference. Other angular positions w.r.t. this particular direction can then directly be determined from the phase difference between the two received signals (see figure 7.13). This principle is used, e.g., in the VOR (VHF omni-range) in aircraft navigation.

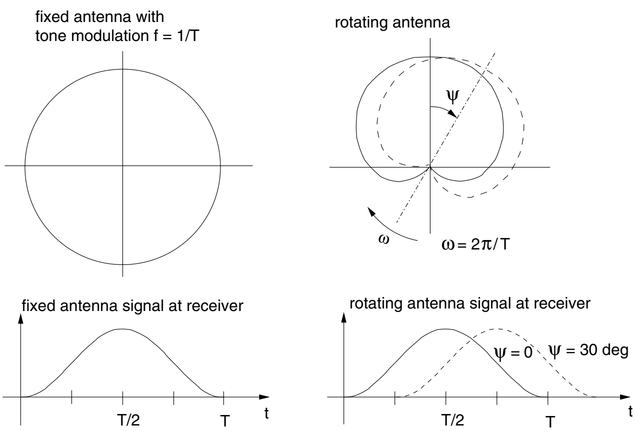


Figure 7.13. Relative attitude measurement through fixed and rotating antenna pattern on target.

**Relative attitude measurement through antenna beams with different tone modulation** Two antennas are radiating their patterns or beams under different angles and with the same carrier, but with different modulation frequencies $f_1$ and $f_2$. A receiver with one channel for each carrier, located exactly in the middle between the centre lines of the two patterns, will receive both transmissions with the same amplitude. At the sides of the middle line between the two patterns, the amplitude of one of the modulation frequencies will become lower and the other one will become stronger. The angular position can thus be determined from the ratio of the amplitudes of the received modulation frequencies $f_1$ and $f_2$. Two cases are shown in figure 7.14: the first is the superposition of two dipole antennas, and the second shows the arrangement of two narrow beam antennas. The first can be used unambiguously in one quadrant. The second can be used only within a small angular range, but with higher accuracy. This type of angular position measurement is used, e.g., in the instrument landing system (ILS) for aircraft.

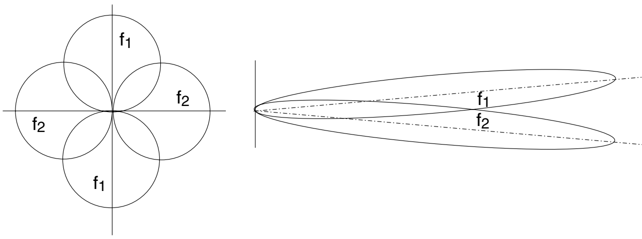


Figure 7.14. Relative attitude measurement through antenna beams on target with different modulation.

### 7.2.3 Measurement environment, disturbances

The performance of a sensor is usually described in terms of resolution, bias and noise. There are, however, other disturbances and effects which affect the performance but are neither caused inside the sensor itself nor are inherent to the measurement chain. They may be caused by effects of the environment of the measurement process and may be present in certain types of environment though not in others. For such external effects, the term 'measurement environment' is used here.

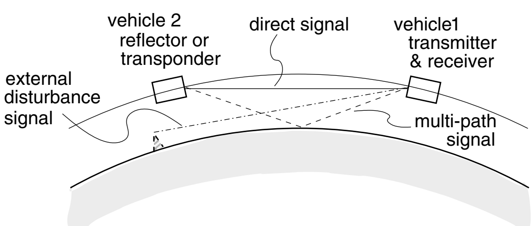


Figure 7.15. Multi-path signal reflected by Earth and external disturbances.

The major part of the disturbances due to the measurement environment are caused by one of the following effects:

- Multiple reflections of the transmitted signal by structural elements on transmitter spacecraft, resulting in the transmission of multiple or blurred target signals.
- Multi-path effects, i.e. signals arriving at the receiver via multiple paths due to reflection or refraction of the electro-magnetic waves by external bodies, e.g. reflections of transmitter or transponder signals by Earth and/or ionospheric layers; refraction and delays of signal by ionospheric and atmospheric layers; multi-path reflections of transmitter or transponder signal by different surfaces on the target spacecraft; multi-path reflections of the received signal by different surfaces on the receiver spacecraft.
- Shadowing by obstacles in the transmission direction due to structural elements on either transmitter or receiver spacecraft.
- Interference by signals transmitted from other sources using the same frequencies.

Some of the effects are more pronounced when the distance to the target is large and the returning signal is very weak. The last type of disturbance, i.e. signals from other sources, could play a role in such a case. Also, multi-path disturbances by the Earth will be more pronounced at long distances. On the contrary, multi-path and shadowing problems by the target structure are more pronounced in the close vicinity of the target.

Disturbances caused by reflections of the signal by the structure around the transmitting antenna can be avoided by proper design of the antenna and of the vehicle. Disturbances by external sources using the same frequency can of course be avoided by use of frequencies dedicated to a particular mission or application. An application of the above-mentioned passive corner-cube reflector would define a reference point on the target, which can be distinguished from all other spurious reflections by the power of the signal. As discussed above, a transponder on the target would improve the discrimination of the direct signal from spurious reflections and refractions by the target vehicle structure, but would require additional active equipment and power on the target side.

### 7.2.4 General assessment of RF-sensor application

Radio-frequency sensing devices have been used in all rendezvous missions so far for the measurement of range and direction or position. Examples are the rendezvous radars, used in the American rendezvous missions from Gemini up to the Space Shuttle, and the radio-frequency system 'Kurs' used by the Russian (Soviet) space programme. The Russian 'Kurs' system, which will be addressed as an example for an RF-sensor system in more detail in the following section, combines a number of principles for range and angular measurement that have been described above. Satellite navigation is a particular form of RF-sensing, applying time-of-flight and phase measurement principles to signals transmitted by a set of navigation satellites. Because of its particular conditions, which are very different from the RF-sensor principles discussed so far, and because of its importance for future rendezvous missions, it will be treated separately in section 7.3.

The limitations of the operational ranges of sensors for rendezvous missions have been discussed in section 5.3.2 in the context of the approach strategy drivers, and an overview of range vs. accuracy has been given in figure 5.10. In addition to the emitted power, the maximum range of RF-sensors depends on the aperture of the antennas. The effective aperture or effective area of an antenna is

$$A_{\mathrm{e}} = \frac{D\lambda}{4\pi}$$

where $D$ is the directivity of the antenna. This provides the relationship between the frequency and the size of an antenna. Assuming a receiving antenna at the range $R$ and using the above relation for the effective area of the receiving antenna, Eq. (7.12) can be expanded to become (Kayton and Fried 1997)

$$\frac{\text{received power}}{\text{transmitted power}} = \frac{A_{\mathrm{re}} A_{\mathrm{te}}}{R^2 \lambda^2} \tag{7.25}$$

where $A_{\mathrm{re}}$ is the effective area of the receiving antenna $A_{\mathrm{te}}$ is the effective area of the transmitting antenna and $R$ is the range between antennas and $\lambda$ is the wavelength.

This shows that with fixed antenna areas the received power increases with the square of the frequency. The consequence is that very high frequencies (gigahertz range) have to be used to minimise mass and power. Equations (7.12) and (7.25) also show that eventually there will be, for RF-measurement systems (with the exception of satellite navigation systems, see the next section), a limitation of the maximum operational ranges due to the limitation of available power.

The typical operational range of RF-sensors is the long and medium range of the approach, whereas the very short range would require very high effort to mitigate disturbances and provide the required performance. As for medium and long ranges, the transmitted signal must still be sufficiently strong (with the above addressed consequences on power and antenna size), the RF-sensor techniques described above tend to have a comparatively high power consumption and mass.

It has been demonstrated above that for all navigation parameters required during a rendezvous mission, i.e. range, LOS, range-rate, and relative attitude, an RF-measurement principle is available. In the early development of automatic onboard rendezvous systems, when no alternatives were available, all sensor design was based on RF-techniques (see section 7.2.5). However, as a result of the development of new techniques and technologies, in many cases either measurement performance or mass and power consumption are nowadays more advantageous with other sensor principles. This is true in the long and medium range, mainly for satellite navigation, and in the short range for optical sensors, which are described in the subsequent sections 7.3 and 7.4.

### 7.2.5 Example: the Russian Kurs system

The Kurs system has been used for rendezvous navigation of the Russian Soyuz and Progress vehicles for a long time, first for approaches to the Russian space station Mir, and then to the ISS. Kurs is an example of the combination of various RF-sensor principles into one navigation system. The Kurs system is designed to provide all required navigation measurements during the entire approach from a few hundreds of kilometres down to contact. A short overview of its functions will be given here, since this system is, so far, the only sensor system used in automatic rendezvous and docking missions, and it is going to be used by Russia for many years to come. It can, therefore, be seen as a standard against which newer technologies can be evaluated. The following description is based on printed sources (Suslennikov 1993; *Data Book: Service Module 2000; Data Book: Soyus/Progress 2000*) and on updates (Semyachkin 2001) provided in a letter to the author, reflecting the state of design in 2001.

The Kurs system includes the following functions:

- Identification of the hemisphere of the target direction by two omni-directional antennas to permit the chaser docking port side to be directed into the hemisphere of the target position.
- Identification of the target direction within this hemisphere by a large angle scanning antenna.
- Range measurement based on the shift of a phase modulated signal during the travelling time from chaser to the target and back to the chaser, or vice versa.
- Range-rate measurement based on the Doppler shift of the carrier frequency.
- More precise LOS tracking in azimuth and elevation of the target by a scanning antenna in a $\pm 15$ deg angular range. (In the original design of Kurs, an additional measurement of the LOS rate about the chaser $y$- and $z$-axes was made by gyros mounted on the gimballed antenna (Suslennikov 1993).
- Measurement in the proximity phase ($\leq 200$ m) of relative attitude in pitch and yaw through evaluation of the scan beam pattern transmitted by the scanning antenna on the target and received by the fixed antenna on the chaser, and of LOS angles.
- In the original design, measurement in the proximity phase of the relative roll angle by tracking of antennas, at the circumference of the target, which are transmitting with different frequencies (Suslennikov 1993). This design has been changed: the roll angle is now calculated in the control system of the onboard computer complex from the other information available (Semyachkin 2001).

The Kurs system operates in the S-band using wavelengths of the order of 10 cm, with both continuous wave mode and bi-phase (0–180 deg) modulated signals. It comprises active functions on both chaser and target vehicles, as shown in figures 7.17 and 7.18. The navigation parameters and their measurement range are as follows:

- coarse LOS angles: $\psi_0$, $\vartheta_0$: $\pm 180$ deg, during acquisition;
- range $R$: unambiguous in the range 0–100 km, beyond 100 km repeating, i.e. at 180 km the measurement is 80 km;
- range-rate $\dot{R}$: 400 m/s, all ranges after acquisition;
- LOS angles $\psi_\Gamma$, $\vartheta_\Gamma$: $\pm 15$ deg, all ranges after acquisition;
- LOS angles $\gamma_\psi$, $\gamma_\vartheta$: $\pm 15$ deg, in the proximity phase $\leq$200 m;
- relative attitude $\psi_\Pi$, $\vartheta_\Pi$: $\pm$ 30 deg, in the proximity phase $\leq$ 200 m.

In the original design, the relative roll angle was also measured in the proximity phase ($\leq$200 m), and the LOS angular rates $\Omega_y$, $\Omega_z$ were measured in all ranges after acquisition by gyros on the antenna platform (Suslennikov 1993). In the present design, the gyros have been omitted, and angular rate is no longer measured directly (Semyachkin 2001). The antennas used for these measurements are shown in figure 7.16. A short description of their functions is given in the following.

### Antennas on the chaser vehicle

**A1, A2** These are omni-directional antennas which transmit the frequency $f_1$ generated by the chaser and receive the frequency $f_2$ generated by the target. The antennas are used for acquisition to determine the hemisphere of the target position. After acquisition they transmit and receive the signal used in the range and range-rate determination process.

**A3** This is a wide-angle mechanical scanning antenna with a special beam pattern and a scanning cone angle of 200 deg. It receives the frequency $f_2$ transmitted by the target and is used for coarse direction finding of the target position, i.e. providing the information for determination of the coarse LOS angles $\psi_0$, $\vartheta_0$ w.r.t. the $x$-axis of the vehicle. Together with antennas A1 and A2, it is used in the acquisition process to point the chaser $x$-axis toward the target.

**A4** This is a fixed antenna with an electronic scanning cone angle of 30 deg (Semyachkin 2001). (In the original design, it was mounted on a gimbal system with $\pm 15$ deg freedom (Suslennikov 1993).) It transmits the interrogation frequency $f_1$ and receives, after acquisition, the frequency $f_2$ transmitted by antennas B1 and B2 on the target and, in addition, in the proximity phase ($\leq$200 m) the frequencies $f_3$ and $f_4$ transmitted by antennas B3, B4 and B5 on the target. The frequencies $f_1$ and $f_2$ are used for range ($R$), range-rate ($\dot{R}$) and LOS angles ($\psi_\Gamma$, $\vartheta_\Gamma$) tracking. The frequencies $f_3$ and $f_4$

are used for roll determination by LOS angles $\gamma_\psi$ and $\gamma_\vartheta$ (Semyachkin 2001).(In the original design these antennas were used for direct roll measurements, and, as already mentioned, two gyros mounted on the gimballed platform of the antenna delivered the LOS angular rates $\Omega_y$ and $\Omega_z$ (Suslennikov 1993).)

To establish a precise measurement axis, electronic beam switching is performed, which in turn establishes antenna sub-beams somewhat similar to the ones shown in figure 7.14, except that the different sub-beams are not separated by frequency but by time. If the antenna measurement axis is directly pointing toward the target, all sub-beams will receive the same signal amplitude.

**A5** This is a fixed antenna with a narrow beam characteristic, receiving the frequency $f_4$ transmitted by antenna B5 on the target vehicle. A5 is used in the proximity phase ($\leq$200 m) for measurement of LOS angles $\psi_\Gamma$ and $\vartheta_\Gamma$. From the amplitude information of the received signal, the relative attitude angles ($\psi_\Pi$, $\vartheta_\Pi$) are derived.

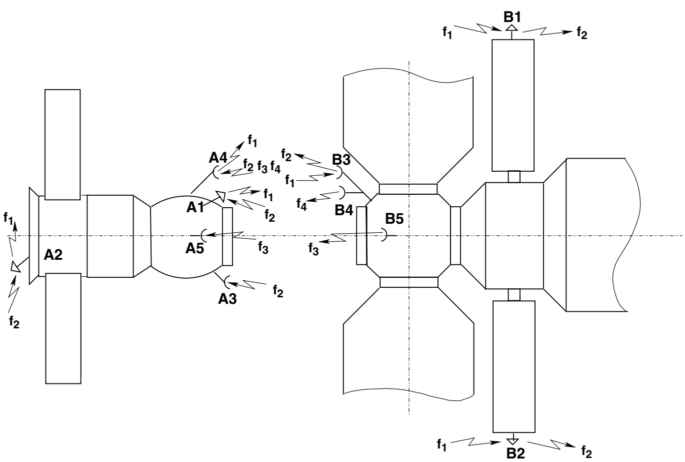


Figure 7.16. Location of Kurs antennas on Progress and Mir.

## Antennas on the target vehicle

**B1, B2** B1 and B2 are omni-directional antennas which transmit the frequency $f_2$ generated by the target and receive the frequency $f_1$ generated by the chaser. In function and performance they correspond to the antennas A1 and A2 on the chaser vehicle.

**B3** B3 is a fixed antenna with a $\pm$30 deg antenna characteristic. In the proximity phase ($\leq$200 m) the transponder of the target switches to antenna B3 for transmitting frequency $f_2$. During this phase this antenna also receives frequency $f_1$ transmitted by the chaser and is used for determination of range and range-rate on the target side.

**B4** The signal of antenna B4 is mainly used in the last 30 m for improved range measurement between chaser and target. B4 is a fixed antenna with a ±20 deg beam characteristic transmitting a separate frequency $f_4$.

**B5** B5 is a motor driven conical scanning antenna, rotating with 700 rpm (11.66 Hz) and describing a cone with a half-angle of 30 deg. The antenna transmits a frequency $f_3$ with an amplitude modulation at 11.66 Hz. The principle of measurement is somewhat similar to the one described in figure 7.13, except that the rotating pattern is not a cardioid: the 11.66 Hz amplitude modulated signal is compared with the amplitude variation of the carrier received by antenna A5 on the chaser. If the carrier signal is constant, the chaser is aligned with the target. If the carrier has an amplitude, the amplitude and phase difference with the modulation can be evaluated to determine the relative attitude.

### Hardware of the Kurs system

The equipment on the chaser vehicle side (Soyuz or Progress), called the 'interrogator' since it contains most of the active measurement functions, is shown schematically in figure 7.17. The antennas are switches by the 'commutator' as selected by the 'logic unit' (not shown). The engagement of antennas also depends on mission progress and is controlled, as for all other Kurs equipment, by inputs from the onboard computer. The scan control functions are not shown in the figure.

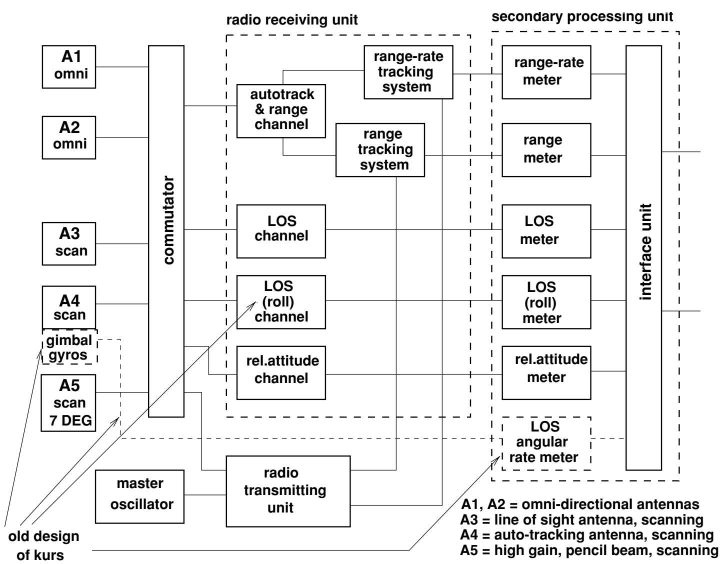


Figure 7.17. Functional block diagram of Kurs 'interrogator' equipment.

The information required for determination of range, range-rate, LOS angles and relative attitude are extracted in the 'radio receiving unit' from the signals received by the various antennas via the carrier frequencies $f_2$, $f_3$ and $f_4$. From these extracted signals the output navigation parameters range, range-rate, LOS angles and relative attitude are calculated in the 'processing unit' and are sent to the onboard computer of the vehicle for use in the GNC system and in the crew displays.

The 'radio transmitting unit' produces the carrier frequency $f_1$ and the bi-phase modulation for the interrogation signal to be transmitted to the target. The transmitted signals are also provided as a reference to the range and range-rate tracking loops in the 'radio receiving unit'.

The equipment on the target (Mir or ISS) is shown schematically figure 7.18. In addition to the transponder function proper, i.e. re-transmission of the interrogation signal on frequency $f_2$ back to the chaser, it has to provide the frequencies and modulations $f_4$ and $f_3$ to be transmitted by antennas B4 and B5. For antenna B5 the motorised drive for the conical scan also has to be provided. Further, the Kurs system on the target includes the range and range-rate measurement loops as the chaser system. The output is provided, via the 'processing unit', to the displays for the target crew.

The following values have been given for the mass and power consumption of the Kurs equipment on chaser and target (Suslennikov 1993; *Data Book: Soyus/Progress* 2000; *Data Book: Service Module* 2000; Semyachkin 2001):

total mass of redundant equipment on chaser side $\approx$ 85 kg

total power consumption on chaser side $\approx$ 270 W

total mass of redundant equipment on target side $\approx$ 80 kg

total power consumption on target side $\approx$ 250 W

### Operation of antennas during rendezvous

At a range of about 200 km, the antennas B1 and B2 on the target will start to transmit the unmodulated frequency $f_2$, alternating between the two antennas at a rate of 1 kHz. The two antennas A1 and A2 on the front (docking port) and back-sides of the chaser vehicle are also switched at 1 kHz, receiving alternating the $f_2$ beacon signal of the target. The difference in strength of the signal received in A1 and A2 determines in which hemisphere the target is located. If necessary, an attitude manoeuvre is initiated to ensure that the chaser docking port is within the hemisphere of the target location. As the target is now located in the reception range of the scanning antenna A3 (200 deg cone), its pointing direction can be determined more precisely and the chaser can be moved to place the target into the reception range of the main tracking antenna A4.

The chaser Kurs system starts now to interrogate the target on carrier frequency $f_1$ with a bi-phase modulated signal at a modulation frequency of 800 Hz. The target

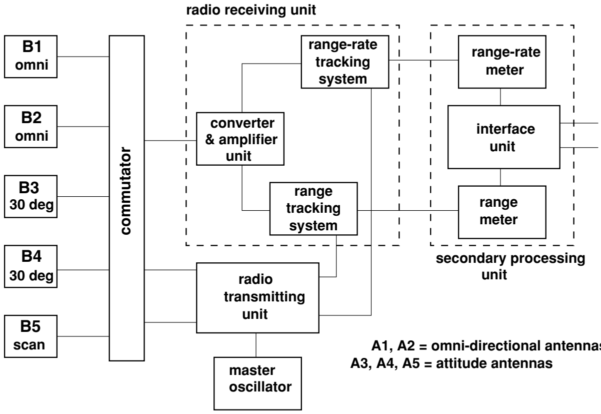


Figure 7.18. Functional block diagram of Kurs 'transponder' equipment.

system responds via antennas B1 and/or B2 by sending back the modulation signal on a different carrier $f_2$. The signal, which has been two times phase shifted over the range $R$, can be evaluated concerning the range, making use of the modulation signal (see Eq. (7.5)) and concerning the range-rate, making use of the carrier frequency (see Eq. (7.18)). The same process is also performed on the target, so that range and range-rate information is available on both vehicles.

During the fly-around or closing phase between 400 m and 200 m, the chaser will be aligned to the docking axis of the target. When all of the frequencies transmitted by the target alignment antennas, i.e. $f_2$ by antenna B3, $f_4$ by antenna B4 and $f_3$ by antenna B5, are received by their counterparts A4 and A5 on the chaser, station keeping will be performed at a range of $\approx$200 m.

During the subsequent final approach (from 200 m to 20 m) chaser antenna A4 will track target antenna B3 and chaser antenna A5 will track target antenna B5. B3 transmits in this range the Kurs transponder signals used to obtain range, range-rate and LOS angle information. B5 provides the reference for relative attitude detection in pitch and yaw. During the last 30 m of approach antenna A4 on the chaser receives in addition the signal from antenna B4 on the target, which is used together with the signal from B3 to determine the range by angle $\gamma_\vartheta$.

# 7.3 Absolute and relative satellite navigation

## 7.3.1 Description of the navigation satellite system setup

As in the previous section, only the basic measurement principles required for a general understanding of absolute and relative navigation via navigation satellites will be described here. For more detailed information, readers are referred to the literature on the subject, such as Ackroyd & Lorimer (1990), Scott *et al.* (1995), Kaplan (1996), Dye & Baylin (1997), Kayton & Fried (1997).

Satellite navigation systems are radio navigation systems based on signals transmitted by a set of satellites orbiting the Earth. They provide navigation information to the user through measurement of range and range-rate between a user receiver and a subset of these navigation satellites. Satellite navigation systems are generally composed of three segments:

(1) a space segment, including the navigation satellites as the active partners of the user in obtaining the navigation information;

(2) a ground segment, controlling the orbital parameters, the accuracy of onboard time and the accuracy of the navigation messages broadcast by the navigation satellites;

(3) a user segment, consisting of the navigation receivers, the locations of which are to be determined. More than one receiver may be used in cooperation to improve relative navigation accuracy between those receivers (see DGPS and RGPS).

At the time of writing, two major navigation satellite systems are deployed:

- the Global Positioning System (GPS), developed and operated by the United States of America;
- the Global Orbiting Navigation Satellite System (GLONASS), developed and operated by Russia.

Because of the importance satellite navigation has gained in all areas of terrestrial navigation for land vehicles, ships and aircraft, these systems will be further developed and enhanced. At the time of writing, within the frame of the international 'Global Positioning and Navigation Satellite System' (GNSS-1) programme, overlay systems by geostationary satellites are under development, i.e. the American 'Wide Area Augmentation System (WAAS), the 'European Geostationary Overlay Service' (EGNOS) and the Japanese 'MTSAT Satellite Based Augmentation System' (MSAS). These three systems will provide a seamless geostationary overlay service to the GPS and GLONASS systems and were planned, at the time of writing, to be available in the middle of the first decade of the twenty-first century. Further steps toward a GNSS-2 programme with new satellite configurations are being planned.

### Setup of the space segment

**GPS** The American GPS space segment nominally consists of 24 operational satellites (the satellites are also called 'Navstar') in near circular orbits with an altitude of approximately 20 180 km (ARINC 1999). The satellites have an orbital period of 12 h, i.e. they make two revolutions per day, thus passing (due to the rotation of the Earth) over the same location once each day (i.e. every 23 h 56 min). There are four satellites

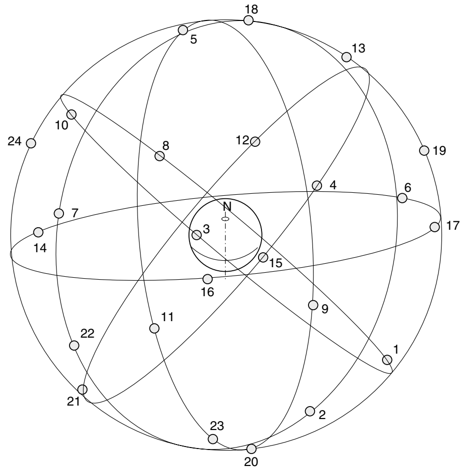


Figure 7.19. GPS satellites in orbit.

on each of the six orbital planes. All orbital planes have an inclination $i = 55$ deg, with their nodes separated by a RAAN angle of 60 deg. Due to disturbances, in particular by the oblateness of the Earth ($J_2$-effect), the nodes of these orbits will drift with time. The spacing of the four satellites in each of the orbital planes is not uniform. It is arranged such that a minimum of five satellites will be available to a user at any position on the Earth and at any time.

The Navstar satellites transmit on two L-band frequencies, i.e. on 1575.42 MHz and 1227.60 MHz, broadcasting a navigation message which includes pseudo-random number (PRN) codes and other information. The latter information includes the satellite identification and information on the orbital characteristics of each satellite and on its onboard clock.

**GLONASS** The Russian GLONASS space segment also nominally consists of 24 operational satellites, which are, however, arranged in three orbital planes separated by 120 deg. There are eight satellites per plane equidistantly arranged, i.e. with a separation of 30 deg. The orbital altitude is 19 130 km and the inclination of each plane is 64.8 deg. The ground track of a satellite repeats itself after 17 orbits, i.e. approximately after 8 days.

The GLONASS satellites transmit carrier frequencies, centred around two L-band frequencies, 1602 and 1246 MHz, with each satellite having its own frequency. GLONASS satellites also broadcast PRN codes, navigation messages etc., but in a slightly different way as compared with GPS.

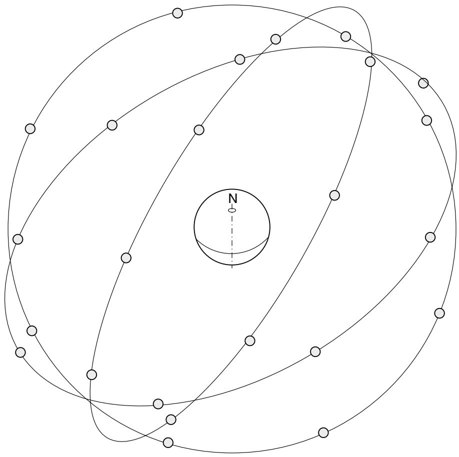


Figure 7.20. GLONASS satellites in orbit.

**Galileo** The next step in the development of a 'Global Positioning and Navigation Satellite System' (GNSS-2) will be the development of a global satellite navigation system by Europe, called 'Galileo'. This new constellation is planned to comprise 27 operational satellites and three spares in circular orbits of 24 000 km altitude, arranged in three orbital planes with 55–60 deg inclination. Full inter-operability with GPS and GLONASS is envisaged. An initial service is foreseen by 2008 with full operational capability by 2010. Positioning accuracies of down to 4 m are envisaged with the Galileo service.

### Setup of the ground segment

To control a navigation satellite system, four ground antenna stations are needed at suitable locations on the Earth. When the positions of the stations are precisely known and the time at the stations is precisely synchronised, the navigation equations discussed below for the user segment can be used in an inverse way to determine exactly the location or the orbit ephemerides of the navigation satellites. Because of the orbital disturbances caused by the Earth, the Sun and the Moon, the orbital parameters of all satellites need to be measured, and forecasts of their development with time need to be calculated continuously. At regular intervals the navigation messages broadcast by each navigation satellite need to be updated accordingly. Furthermore, the clocks on the navigation satellites need to be monitored and corrected at regular intervals. The complete ground segment setup will therefore consist of:

- at least four monitoring stations with precisely located reception antennas and with high performance receivers;

- a master control station performing the calculations, generating the uplink data, controlling the time synchronisation and monitoring the links with monitoring and transmitting stations;
- a number of transmission stations to uplink commands and data to the navigation satellites.

### 7.3.2 Navigation processing at the user segment

**Range measurement**

To measure the range between navigation satellites and user by the 'time-of-flight' method (see section 7.2.1), the time at transmission of the signal by the navigation satellites must be known. Further, in order to re-constitute the position of the user in a particular coordinate system, the position of the navigation satellite in this system must be known. This requires that the navigation satellites broadcast continuously their position or their orbit ephemerides and time marks as reference, and that the clocks of the user receiver and the navigation satellites are synchronised. From time and orbit ephemerides, the actual position of the satellites at the time reference can then be calculated, and the range can be obtained from the travel time $t_t$ and the speed of light $c$.

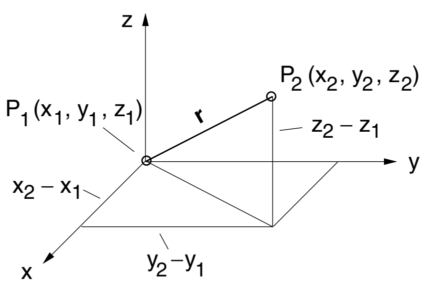


Figure 7.21. Relations for pseudo-range calculation.

As the user receiver's clock will not be fully synchronised with that of the transmitter, the measured range between user and navigation satellite is

$$p = c \cdot (t_1 + t_{\text{bias}} - t_2) = r_{2,1} + c \cdot t_{\text{bias}} \tag{7.26}$$

where $c$ is the velocity of light and $t_t = t_2 - t_1$ is the travel time between point $P_2$ (navigation satellite) and $P_1$ (user), and the term $t_{\text{bias}}$ is the unknown bias of the user clock w.r.t. the navigation satellite clock. Because of this additional unknown, the range $r$ measured by this method is not the real geometric distance $r_{2,1}$ between the user and the navigation satellite and is, therefore, called the 'pseudo-range'. If the position of the transmitter is known, the coordinates of position of the user can be obtained from the following relation (see figure 7.21):

$$r_{2,1} = \sqrt{(x_2 - x_1)^2 + (y_2 - y_1)^2 + (z_2 - z_1)^2} \tag{7.27}$$

where $x_1, y_1, z_1$ and $x_2, y_2, z_2$ are the position coordinates of $\mathrm{P}_1$ and $\mathrm{P}_2$ in an inertial Earth-centred Cartesian coordinate system. Whereas a three-dimensional position can generally be determined by the range measurement to three known targets, the bias can be eliminated by the pseudo-range measurement w.r.t. a fourth navigation satellite, yielding four equations for the four unknowns:

$$\begin{aligned}
(x_{\mathrm{n1}} - x_{\mathrm{u}})^2 + (y_{\mathrm{n1}} - y_{\mathrm{u}})^2 + (z_{\mathrm{n1}} - z_{\mathrm{u}})^2 &= c^2 \cdot (t_{\mathrm{u1}} + t_{\mathrm{bias}} - t_{\mathrm{n1}})^2 \\
(x_{\mathrm{n2}} - x_{\mathrm{u}})^2 + (y_{\mathrm{n2}} - y_{\mathrm{u}})^2 + (z_{\mathrm{n2}} - z_{\mathrm{u}})^2 &= c^2 \cdot (t_{\mathrm{u2}} + t_{\mathrm{bias}} - t_{\mathrm{n2}})^2 \\
(x_{\mathrm{n3}} - x_{\mathrm{u}})^2 + (y_{\mathrm{n3}} - y_{\mathrm{u}})^2 + (z_{\mathrm{n3}} - z_{\mathrm{u}})^2 &= c^2 \cdot (t_{\mathrm{u3}} + t_{\mathrm{bias}} - t_{\mathrm{n3}})^2 \\
(x_{\mathrm{n4}} - x_{\mathrm{u}})^2 + (y_{\mathrm{n4}} - y_{\mathrm{u}})^2 + (z_{\mathrm{n4}} - z_{\mathrm{u}})^2 &= c^2 \cdot (t_{\mathrm{u4}} + t_{\mathrm{bias}} - t_{\mathrm{n4}})^2
\end{aligned} \tag{7.28}$$

In these equations the subscript ‘u’ denotes the user and the subscript ‘n’ denotes the navigation satellites. The positions $x_{\mathrm{n}}, y_{\mathrm{n}}, z_{\mathrm{n}}$ of satellites 1–4 can be calculated from the orbital data of the navigation message, which is broadcast by each of the satellites. The times $t_{\mathrm{u}i}$ are measured by the user receiver. The receiver bias is the same in all measurements. Eqs. (7.28) are non-linear and thus need to be linearised, e.g. by expansion into a Taylor series about an estimated position, and iteratively solved to arrive at sufficiently accurate solutions (an example for the derivation of such a solution is given in Kaplan (1996).

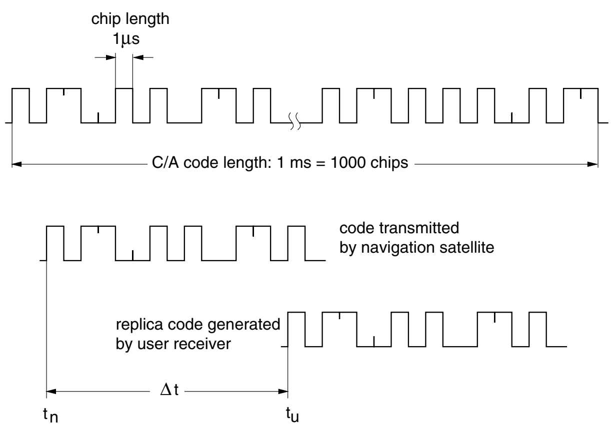


Figure 7.22. Pseudo-random number (PRN) sequence for coarse acquisition (C/A) code.

The next important question to be explained is, how can the user receiver continuously measure the time differences $t_{\mathrm{u}i} - t_{\mathrm{n}i}$? The navigation satellites continuously transmit digital binary codes. These codes are called pseudo-random number (PRN) codes, because of their apparently random sequence of zeros and ones. They have, however, a certain length, after which they are repeated, and can therefore be compared to a melody which is continuously repeated. These PRN codes (or digital melodies) are generated and transmitted by the navigation satellite, with each navigation satellite broadcasting its own tune (GPS) or the same melody but on a slightly different carrier frequency (GLONASS). The user receiver can identify a navigation satellite either by its navigation message 'melody' (GPS) or by the carrier frequency (GLONASS). The receiver has a replica of the (civilian) PRN codes available and can correlate the emitted code once it has identified a navigation satellite.

In its navigation message, the navigation satellite also transmits information concerning the time of the transmission w.r.t. the reference time of the navigation satellite and concerning the start on the PRN code sequence. This is necessary because of the range ambiguity over a long distance of a signal, which repeats itself after 1 ms. In an overall travelling distance of about 20 000 km, it will repeat itself about 66 times. With the time of transmission and the code information available, the user receiver can compare the received PRN code with its replica code and can determine the shift in time (see figure 7.22) by auto-correlation techniques. With the found $\Delta t$, the pseudo-range can be calculated according to Eq. (7.26). With $\Delta t$ measurements from four navigation satellites, the position can be determined by solving Eqs. (7.28).

Both GPS and GLONASS transmit two types of PRN codes, a 'coarse acquisition' (C/A) code and a 'precision' (P) code. To civil users only the C/A code is accessible. The C/A code is in both cases 1 ms long and constantly repeated. The chip length (length of a '0' or '1') of the C/A code is approximately 1 $\mu$s. The P code is extremely long, e. g. for the GPS it is 1 week, and is repeated after that period. Its chip length is 0.1 $\mu$s. Because of the exclusively military use of the P code, it is not necessary to discuss it here in more detail.

According to Eq. (7.4) the carrier phase can also be used for range measurement. Because of the large distance to the navigation satellites and the high frequency used, there will be a very large number of cycles over the range where the same phase angle occurs that is measured at the receiver. This will make it more difficult to establish the total range. The carrier phase measurement can be used, however, (via the Doppler effect) to improve the pseudo-range result (see the sub-section entitled 'Velocity and change-of-range measurement' below).

### Measurement errors

In order to show the principle of the concept, it has been assumed so far that only errors in the clock time of the receiver exist. In reality there are a number of other errors which affect the accuracy of the pseudo-range measurement. Generally, the pseudo-range to a navigation satellite will include the following error components:

$$p = c\,\Delta t + E_{\mathrm{t-rec}} + E_{\mathrm{t-ion}} + E_{\mathrm{t-sat}} + E_{\mathrm{ephem}} + E_{\mathrm{n-rec}} + E_{\mathrm{t-trop}} \tag{7.29}$$

where

$E_{\mathrm{t-rec}}$ = error due to receiver clock bias ($\approx$ 1 m)
$E_{\mathrm{t-ion}}$ = error due to ionospheric delay (depending on user orbit $\approx$ 10 m)
$E_{\mathrm{t-sat}}$ = error due to remaining satellite clock error ($\approx$ 1 m)
$E_{\mathrm{ephem}}$ = error due to navigation satellite ephemeris error ($\approx$ 1 m)
$E_{\mathrm{n-rec}}$ = error due to receiver noise ($\approx$ 0.5 m)
$E_{\mathrm{t-trop}}$ = error due to tropospheric delay ($\approx$ 1 m)

Errors due to multi-path effects and shadowing are not inherent to the measurement process proper and will therefore be discussed later. Another artificial error, which has been introduced for GPS under the name of 'selective availability' will be addressed separately below. Combining all measurement errors, Eq. (7.29) can be written as

$$p = c\,\Delta t\,\sigma_{\mathrm{p}} \tag{7.30}$$

where $\sigma_{\mathrm{p}}$ is the pseudo-range error factor combining all errors listed in Eq. (7.29).

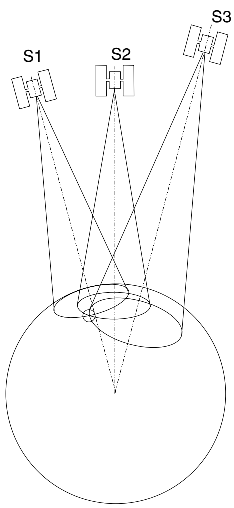


Figure 7.23. Locus of equal distance from navigation satellites.

### Errors due to geometry of constellation

Independently of the above errors, not all visible combinations of four navigation satellites will, for the user, lead to the same position measurement accuracy. If the four satellites selected by the user receiver for position measurement are relatively close together, their loci of range (figure 7.23) will intersect at small angles, leading to poor results in the triangulation. The best result would be obtained in the hypothetical case that, seen from the user, one navigation satellite would be in zenith and the other three around the horizon, separated by 120 deg; this is, of course, not realistic. Generally, the results will improve the farther apart the four satellites are. In order to obtain a quantisation of the effects of the geometric constellation of the selected satellites on the position accuracy result of the user, the concept of a 'geometric dilution of precision' (GDOP) has been introduced. The definition of GDOP can be explained as follows. The total of the standard deviations $\sigma_{\mathrm{tot}}$ relating to the user position and time in Eq. (7.27) (clock bias and geometric constellation effects included) can be expressed as

$$\sigma_{\mathrm{tot}} = \sqrt{\sigma_{x\mathrm{u}}^2 + \sigma_{y\mathrm{u}}^2 + \sigma_{z\mathrm{u}}^2 + \sigma_{\mathrm{ct}}^2} \tag{7.31}$$

where $(x_{\mathrm{u}}, y_{\mathrm{u}}, z_{\mathrm{u}})$ is the position of the user, $\sigma_{x\mathrm{u},y\mathrm{u},z\mathrm{u}}$ is its deviation and $\sigma_{\mathrm{ct}}$ is the deviation due to clock errors. This total error can be defined as the pseudo-range error factor $\sigma_{\mathrm{p}}$ times the effect imposed by the GDOP due to the satellite constellation selected:

$$\mathrm{GDOP} \times \sigma_{\mathrm{p}} = \sigma_{\mathrm{tot}} \tag{7.32}$$

The GDOP factor is defined accordingly as

$$\mathrm{GDOP} = \frac{\sqrt{\sigma_{x\mathrm{u}}^2 + \sigma_{y\mathrm{u}}^2 + \sigma_{z\mathrm{u}}^2 + \sigma_{\mathrm{ct}}^2}}{\sigma_{\mathrm{p}}} \tag{7.33}$$

The calculation of the actual GDOP value from the constellation of the four satellites selected for measurement can be found in the literature; see, e.g., Kaplan (1996) and Kayton & Fried (1997). From the overall concept of a 'geometric dilution of precision' as an indicative factor of the quality of the solutions of Eqs. (7.28), other 'dilution of precision' factors can be established, e.g.

PDOP = position dilution of precision (three dimensions)
TDOP = time dilution of precision

According to the definition of GDOP, the position dilution of precision can be defined as

$$\mathrm{PDOP} = \frac{\sqrt{\sigma_{x\mathrm{u}}^2 + \sigma_{y\mathrm{u}}^2 + \sigma_{z\mathrm{u}}^2}}{\sigma_{\mathrm{p}}} \tag{7.34}$$

A value of PDOP = 6 is considered the limit for useful position results, a value of PDOP = 3 is considered to be good.

### Velocity and change-of-range measurement

Measuring the Doppler shift of the carrier frequency provides information on the velocity and on the change of position (for the basic measurement principle see Eq. (7.6) and figure 7.7). The received frequency is, according to Eq. (7.7),

$$f_{\mathrm{R}} = f_{\mathrm{T}} \left(1 - \frac{\dot{r}}{c}\right)$$

where $f_{\mathrm{T}}$ is the frequency transmitted by the navigation satellite, $c$ is the speed of light and $r$ is the distance to the user. The range-rate is accordingly

$$\dot{r} = \frac{c}{f_{\mathrm{T}}}(f_{\mathrm{R}} - f_{\mathrm{T}}) \tag{7.35}$$

or in terms of the wavelength $\lambda_{\mathrm{T}}$ of the transmitted frequency

$$\dot{r} = \lambda_{\mathrm{T}}(f_{\mathrm{R}} - f_{\mathrm{T}}) \tag{7.36}$$

The measured range-rate, $\dot{r}_{\mathrm{n,u}}$, is the difference between the velocity component in the range direction of the navigation satellite $v_{\mathrm{rn}}$ and the velocity component in the range direction of the user receiver $v_{\mathrm{ru}}$. As the velocity components of the navigation satellite can be estimated from the orbit ephemeris, the velocity of the user receiver in the range direction can be calculated from

$$v_{\mathrm{ru}} = v_{\mathrm{rn}} - \dot{r}_{\mathrm{n,u}} \tag{7.37}$$

The position of the navigation satellite can also be derived from the orbit ephemeris (navigation message), and the position of the user receiver is known from the pseudo-range calculations. From these values, the direction of the range-rate vector can be derived and the $x$-, $y$- and $z$-components of the velocity can be calculated.

The change in range can be obtained by integration of Eq. (7.35) or (7.36):

$$\Delta r = \int \dot{r}_{\mathrm{n,u}} \mathrm{d}t$$

$$\Delta r = \lambda_{\mathrm{T}} \int (f_{\mathrm{R}} - f_{\mathrm{T}})\, \mathrm{d}t \tag{7.38}$$

which can be obtained by counting the difference of the number of cycles between the received frequency and the known carrier frequency over a fixed period of time; this has lead to the term 'Integrated Doppler count',

$$N_{\mathrm{Da}} - N_{\mathrm{Di}} = \int_{ti}^{ta} (f_{\mathrm{T}} - f_{\mathrm{R}})\, \mathrm{d}t \tag{7.39}$$

where $N_{\mathrm{D}a}$ is the count at the time $t_a$ and $N_{\mathrm{Di}}$ is the initial count at the time $t_{\mathrm{i}}$. The change in pseudo-range is then

$$\Delta r = (N_{\mathrm{D}} - N_{\mathrm{Di}})\lambda_{\mathrm{T}} - E_N \lambda_{\mathrm{T}} \tag{7.40}$$

where $E_N$ is the sum of all errors in this measurement, comprising those presented in Eq. (7.29) and other errors due to the measurement environment (see section 7.3.4). Because one cycle of the carrier frequency ($\leq$1 ns) is much shorter than one chip of the PRN code (1 ms), the resolution of the change of range is more than two orders of magnitude better than that of the absolute range. According to the wavelength of the carrier, one cycle corresponds to a change of range $\Delta r = \lambda_{\mathrm{T}}$ of

$\lambda_{\mathrm{T}} = 0.1903$ m for GPS L1-frequency
$\lambda_{\mathrm{T}} = 0.2442$ m for GPS L2-frequency
$\lambda_{\mathrm{T}} = 0.1873$ m for GLONASS L1-frequency
$\lambda_{\mathrm{T}} = 0.2408$ m for GLONASS L2-frequency

A large part of the errors of both the pseudo-range and the Doppler measurements consist of noise. Because of the iterative techniques used to solve the navigation equations and used in order to minimise the noise of the navigation solutions, all GPS and GLONASS receivers make use of recursive Kalman filter techniques (see section 6.2.1), for the processing of the navigation results. With the computational resources typically available on spacecraft at the time of writing, the time required for convergence of the filter is usually a couple of minutes. This time has to be taken into account when considering the availability of navigation results after initiation of the receiver.

**Selective availability**

After deployment of the initial GPS satellites, it turned out that the navigation results obtained from the C/A code were much better than had been predicted by the designers. In order to protect their military interests, the United States decided for this reason to decrease artificially the C/A navigation accuracy by imposing a feature called 'selective availability' (SA). SA adds a random change to the GPS satellites clocks, which corrupts the reference time for the time-of-flight measurements, and also induces errors into the navigation messages. With SA applied, the following position accuracies can be achieved (Kaplan 1996):

horizontal 100 m (95% probability)
vertical 156 m (95%)

With SA removed, the position accuracies would be improved to (Kaplan 1996):

horizontal 25 m (95%)
vertical 43 m (95%)

For reasons not made public, the US Government decided to discontinue the application of SA with effect from 1 May 2000. The position accuracies which can be achieved with GLONASS are similar to that of GPS without SA.

### 7.3.3 Functional principle of differential GPS and relative GPS

In this section the terms 'differential GPS' (DGPS) and 'relative GPS' (RGPS) are introduced; this is because these relative navigation principles have become widely known under these names. These principles are, however, not specific to GPS, they can be applied in the same way to GLONASS and also to potential future satellite navigation systems, such as Galileo.

In many applications, but in particular in rendezvous type navigation, it is not the absolute navigation w.r.t. some fixed frame which requires the highest precision of the state vector determination, but the relative navigation between a vehicle and a fixed point or between two vehicles operating in relatively close proximity. Using satellite navigation, the relative state vector can be determined by:

(1) relating the absolute measurements of a moving receiver to those of a fixed reference receiver, the position of which is known precisely (DGPS);

(2) the subtraction of the raw measurements of two receivers located at different positions for a number of common navigation satellites (at least four) and using these differential raw data as the measurement input to a navigation filter (RGPS).

In both cases, most errors will be eliminated only if the two receivers are in the vicinity of each other (not more than a few tens of kilometres).

### Differential GPS

Differential GPS is the method most often used in terrestrial applications. There are several possible methods of implementation (figure 7.24):

(a) The *relative coordinates* of a moving receiver B w.r.t. a fixed reference receiver A are simply the difference of the results from Eqs. (7.28), measured at the same time in both receivers. This is the simplest method, which eliminates ionospheric and tropospheric errors in Eq. (7.29), but it leads to elimination of the satellite errors only if the same navigation satellites are used by both receivers.

(b) Reference receiver A calculates the difference between its known position and the instantaneous solution from the GPS measurements. These position corrections are transmitted to receiver B to correct its *absolute position* solution. The error elimination conditions are as in (a).

(c) Reference receiver A calculates, based on the knowledge of its own position, the corrections for the pseudo-ranges to *all* available navigation satellites. The corrections per satellite are transmitted (actually they may be broadcast for general use) to receiver B, which selects the corrections for the navigation satellites it will use to determine its *absolute position*. The advantage of this method is that the moving receiver is free in its selection of navigation satellites.

In methods (a) and (b), if the measurements by the two receivers are made asynchronously, a correction term

$$\Delta \mathbf{r}(\Delta t) = \Delta t(\dot{\mathbf{p}} + \dot{\mathbf{r}}_{\mathrm{c,t}}) \tag{7.41}$$

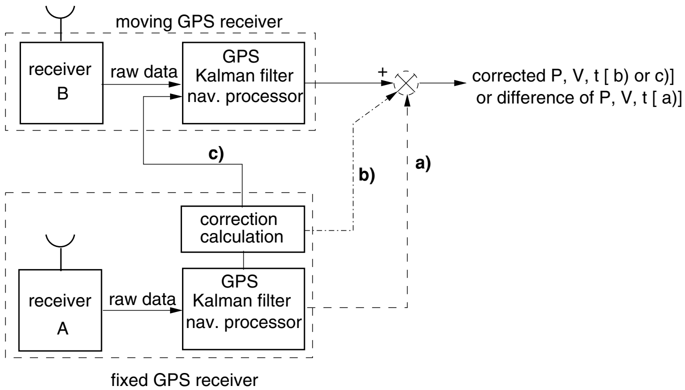


Figure 7.24. Functional principle of differential GPS.

has to be added to Eqs. (7.28) and (7.29), where $\Delta t$ is the time difference between the measurements of chaser and target receivers, $\dot{\mathbf{p}}$ is the vector of the rate of change of the pseudo-range, and $\dot{\mathbf{r}}_{\mathrm{c,t}}$ is the vector of rate of change of the range between chaser and target during the time $\Delta t$. In method (c) the corrections to the pseudo-ranges will change relatively slowly with time, so that asynchronous measurement will not lead immediately to errors.

If the measurements of target and chaser receivers are based on the same navigation satellites, most of the errors in Eq. (7.29), except for the receiver noise, will be cancelled. However, as chaser and target receiver noises are treated independently in the Kalman filters of the chaser and target receivers, they cannot be treated optimally, and also the dynamics of the manoeuvring chaser vehicle cannot be taken into account in an optimal manner.

Since there is no fixed reference receiver available, the DGPS methods for improving absolute navigation are, of course, not possible in space applications. An exception may be the re-constitution of trajectories after flight, where the measurements of a fixed ground receiver may be taken into account for calibration (see section 10.7.2).

## Relative GPS

In relative GPS, the raw data of both receivers, i.e. pseudo-range, Doppler data on the carrier frequency, and reference time, will be processed in the navigation filter of the chaser (see figure 7.25). If both chaser and target GPS receivers make their measurements at the same time, raw data from both receivers can be processed jointly and the linearised equations (7.28) and (7.40) can be solved in the RGPS navigation filter of the chaser for $\Delta$-position and $\Delta$-change of range between chaser and target (see figure 7.26). If the measurements are not performed at the same time, a correction according to Eq. (7.41) has to be applied. Usually, the GPS raw data of chaser and target are delivered with a time tag, so that

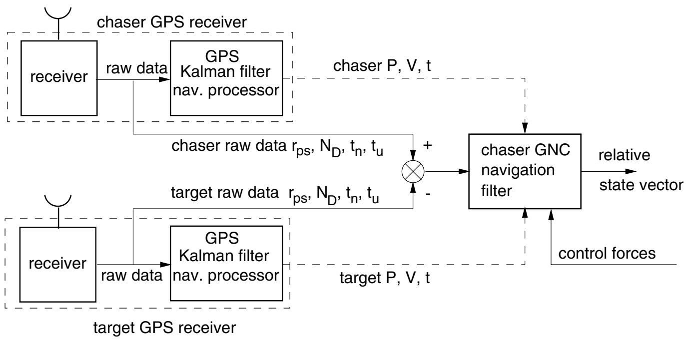


Figure 7.25. Functional principle of relative GPS.

they can be propagated to a common time reference. The single difference between the measurements of receivers A and B to the same navigation satellite i will eliminate satellite and ionospheric error terms in Eq. (7.29), which form the major part of the error budget:

$$\Delta p^{\mathrm{i}}_{\mathrm{A,B}} = p^{\mathrm{i}}_{\mathrm{A}} - p^{\mathrm{i}}_{\mathrm{B}} \tag{7.42}$$

where $\Delta p^{\mathrm{i}}_{\mathrm{A,B}}$ is the new observable, used as the input to the navigation filter of the chaser (see figure 7.26).

To eliminate the clock bias of the receiver in Eq. (7.29), double differences can be processed, i.e. differences between the pseudo-ranges to two different navigation satellites measured by the same receiver and differences between the pseudo-range measurements of the two receivers. Considering receivers A and B and navigation satellites i and j the 'double difference' input to the RGPS navigation filter will be

$$\nabla\Delta p^{\mathrm{i,j}}_{\mathrm{A,B}} = p^{\mathrm{i}}_{\mathrm{A}} - p^{\mathrm{j}}_{\mathrm{A}} - p^{\mathrm{i}}_{\mathrm{B}} - p^{\mathrm{j}}_{\mathrm{B}} \tag{7.43}$$

Because of 'double differencing' all errors except for receiver noise will be eliminated, so the equation can be written as

$$\nabla\Delta p^{\mathrm{i,j}}_{\mathrm{A,B}} = r^{\mathrm{i}}_{\mathrm{A}} - r^{\mathrm{j}}_{\mathrm{A}} - r^{\mathrm{i}}_{\mathrm{B}} - r^{\mathrm{j}}_{\mathrm{B}} + E_{\mathrm{n-A}} + E_{\mathrm{n-B}} \tag{7.44}$$

where $r^{\mathrm{i,j}}_{\mathrm{A,B}}$ are the real ranges of receivers A and B to navigation satellites i and j and $E_{\mathrm{n-A,B}}$ are the receiver noises. A set of four common navigation satellites yields the necessary number of 'double difference' observables $\nabla\Delta p^{\mathrm{i,j}}_{\mathrm{A,B}}$, to solve for the real ranges $r^{\mathrm{i,j}}_{\mathrm{A,B}}$ and to produce the relative position result. The same procedure can be applied to carrier phase measurements, which can be used to smooth the more noisy pseudo-range measurements.

In the general case, each of the two receivers will see a number of navigation satellites, of which only a part will be common to both of them. In the navigation process, the first task is, therefore, to identify the common navigation satellites and select at least four suitable ones for relative navigation processing according to criteria such as GDOP. The raw data for the selected navigation satellites of the two receivers are then corrected for synchronisation of measurement time and subtracted. The accurate calculation of the measurement matrix of the Kalman filter requires knowledge of the absolute position and attitude. However, it may be less accurate than the relative navigation data. The measurements are then fed into the process of state update, gains and covariance computation and state and covariance propagation, as described in section 6.2.1. A simplified block diagram of a navigation filter for RGPS is shown in figure 7.26.

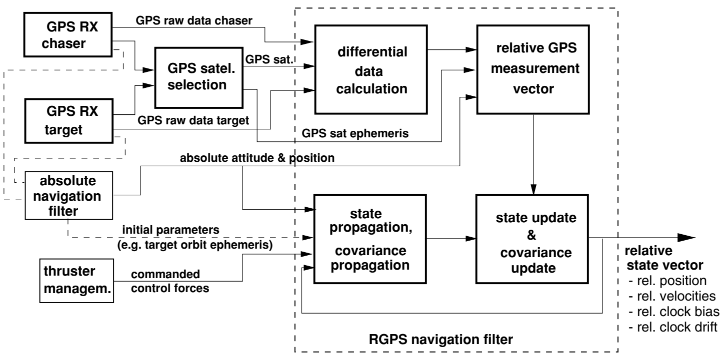


Figure 7.26. Block diagram of a relative GPS navigation filter.

Using this method and with the technology available at the time of writing, the accuracy achievable with RGPS is of the order of 10 m for position and 0.05 m/s for velocity, as compared with about 100 m (30 m without SA) position and 0.5 m/s velocity for absolute GPS. The range of operation of RGPS is limited by two constraints: one being the effectiveness of error cancellation, which decreases with increasing distance between the receivers, and the other being the range of the radio link between chaser and target that is necessary to transfer raw data from vehicle to the other. The maximum useful range may also be limited by the availability of a communication link. Link range may be limited on the far end by the transmitting power available and at short distances by shadowing from the structure of one of the two vehicles.

## 7.3.4 Measurement environment, disturbances

The most important disturbances and limitations of absolute and relative satellite navigation are due to shadowing and multi-path effects. The eventual outcome due to multi-path effects is a distortion of both the code and the carrier of the direct signal of a navigation satellite. The term 'shadowing' is used here for the obstruction of view from a GPS receiver antenna to a navigation satellite by the structure of the other spacecraft. It plays a significant role when the chaser is in the close vicinity of the target, i.e. when the range to the target is of the same order or less than the geometric extensions of the target. For target stations with large rotating solar arrays, such as Mir and the ISS, the overall shadowing characteristics will also depend on the angles of the various solar generator surfaces w.r.t. the local orbital frame. As these surfaces are pointing toward the Sun, shadowing is dependent on the instant location of the navigation satellites to be used, on the position of the vehicles along the orbit (day/night phase), and on the time of year. The actual shadowing conditions can be obtained for a particular mission only by a proper simulation of the chaser and target orbital motion and of the orbital motions of the navigation satellites. At close range, for the most important approach directions, i.e. $+$ or $-$V-bar direction, or below the target on the $+$ R-bar side, the target will mask a part of the hemisphere, large enough that an uninterrupted view of four common satellites is not guaranteed. This is one of the effects which determine the lower limit of operational use of satellite navigation in rendezvous missions.

Multi-path effects due to reflection and refraction of navigation satellite signals by the Earth can affect the function of navigation satellites near to or under the horizon (tangential plane to the actual orbital position) of the receiver (GMV 1997). This effect does not influence the measurements if the antennas of the two vehicles are pointing mainly toward the zenith and are masked for low elevations.

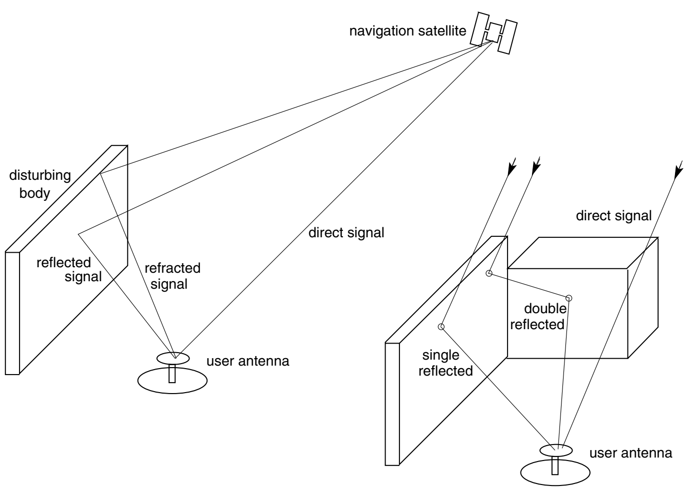


Figure 7.27. Multi-path effects due to external structures.

Multi-path effects by external structures can be caused by the following mechanisms (GMV 1997):

- specular reflections by surfaces,
- diffractions, e.g. by edges.

The amplitude of the diffracted signal is much lower than that of specular reflections. However, GPS antennas are designed for reception of the direct GPS signal, which is right hand polarised. Single reflections from planar metallic surfaces will change to a large extent the signal polarisation from right to left hand. Signals different from right hand polarisation should be strongly attenuated by the GPS antenna. The disturbance effect of single-reflected multi-path signals would, therefore, be low. Typical values for errors by single-reflected or diffracted signals are 5–10 m for pseudo-range and 5 cm for carrier phase. However, if such a signal is reflected a second time, polarisation will change again, from left to right hand. Double-reflected multi-path signals will therefore cause the strongest disturbance effects, which can be 40–100 m in pseudo-range and 2–3 cm in carrier phase (GMV 1997). ESA has observed in a flight experiment peaks of up to 300 m of error in pseudo-range (Ortega *et al.* 1998).

Another error is the so-called 'cycle slip', which occurs when a receiver loses the lock on a navigation satellite, e.g. due to shadowing. From the start of a measurement onward, the cycle count is precisely recorded and related to the start of a PRN code sequence (locking on a satellite). If reception of the satellite transmission is interrupted for a certain time, a 'loss of lock' will occur. On resumption, locking has to be established again. As a result there will be a 'jump' in the measurement data.

### 7.3.5 General assessment of satellite navigation for RVD

Satellite navigation provides a unique capability to determine the absolute position and velocity of a spacecraft in an Earth-centred coordinate frame during all mission phases. Without satellite navigation the absolute state of a space vehicle could be determined only by multiple measurements from ground or on board by complex RF- or astro-navigation. In addition, satellite navigation enables relative measurements of position and velocities between chaser and target, if both vehicles are equipped with appropriate navigation receivers and if the raw data of one of the receivers can be transmitted to the other vehicle. Relative navigation can be performed over relatively large distances between the vehicles (50 km or more) with an accuracy of the order of 10 m for position and 0.05 m/s for velocity, provided a communication link for that range is available. As relative navigation requires a cooperating target with navigation receiver and communication link to the chaser, this type of sensor will not be suitable for, e.g., rescue approaches to incapacitated spacecraft, where one or more of the necessary functions on the target side may have failed.

The range and range-rate measurement accuracy achieved by satellite navigation techniques is independent of the actual range between chaser and target. This is true to a large extent also for relative satellite navigation. The advantage for the rendezvous approach lies in the relatively high manoeuvre precision that can be achieved at large ranges and which reduces the number of manoeuvre iterations necessary (see section 7.1.1). The lower limit of the operational range of satellite navigation for rendezvous missions, given by the relative navigation performance and by the disturbances discussed above, will be a few hundred metres from the target.

In contrast to other RF-sensor techniques, mass and power consumption of satellite navigation receivers are not dependent on the distance between chaser and target. Only for relative navigation is such a dependency given by the power required for the communication link between the two vehicles. A communication link such as this may, however, in practically all cases (except for the approach to an incapacitated spacecraft) also be required for operational reasons. The overall expenditure on power and mass is, for navigation systems based on satellite navigation receivers, considerably lower than for other RF-sensor systems for the same operational range.

## 7.4 Optical rendezvous sensors

In this section two types of optical sensors are considered: scanning laser range finders and camera sensors. Both require optical corner-cube reflectors as interfaces on the target. These two types of sensor principles were developed in the final two decades of the 20th century, precisely for the application in automated rendezvous and docking missions. With the advance of image recognition techniques and other new technologies, it can be expected that in future a larger variety of sensor principles will be both available and suitable for automated rendezvous.

### 7.4.1 Scanning laser range finder

Scanning laser range finder types of sensors (in some publications called ‘telegoniometers’) function according to the same basic physical principles (see section 7.1.2) as radar types of sensors, described in section 7.2. The difference in technology is due to the wavelength of the electro-magnetic signal. The wavelengths used for these types of optical sensors are in present applications in the near infrared range of the order of 1000 nm, depending on the available laser diode technology. The range can be determined either by measuring the time-of-flight (cf. Eq. (7.3) for pulse laser range finder) or by the shift of phase of the returning signal (cf. Eq. (7.5) for continuous wave laser range finder). The direction can be determined by scanning the laser beam and measuring the angle at which a return signal is received, either by guiding the transmitted and received laser signals via two mirrors or by placing the optical head of the laser range finder into a gimbal system, which is oscillating about orthogonal axes (see figure 7.28). The angles of the mirror axes can be read by optical encoders or resolvers to obtain the LOS angles to the target, $\psi$ and $\vartheta$. On the target side, the transmitted laser beam will be reflected back into the direction of the transmitter by optical corner-cube reflectors.

The design and development of laser range finder types of rendezvous sensors has been reported in several publications (NASA 1992; Moebius, Kolk & Manhart 1997; Kolk & Moebius 2000; Luther & Meissner 2000).

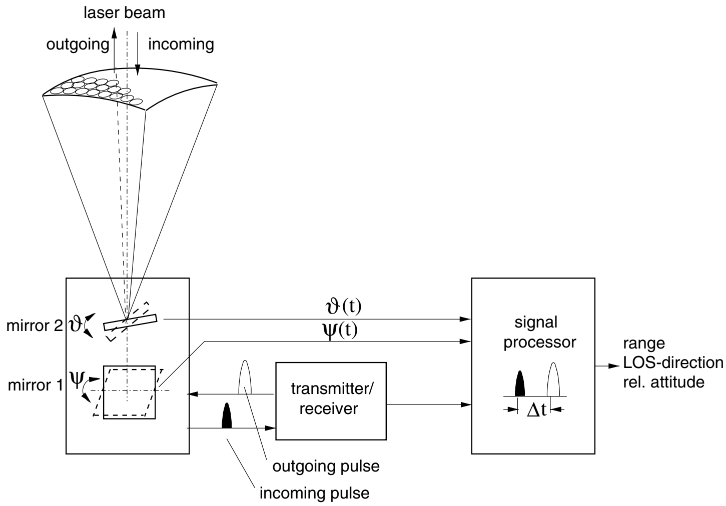


Figure 7.28. Functional principle of a scanning laser range finder.

As in the case of the RF radar, the received power is equal to the transmitted power times the ratio of effective reflector area to the cross section of the transmitted beam times the ratio of the effective receiver antenna area to the cross section of the reflected beam. With the cross section of the transmitted beam given by $\frac{\pi}{4}(R \cdot \varphi_{\mathrm{t}})^2$ and the cross section of the beam reflected by the corner-cubes $\frac{\pi}{4}(R \cdot \varphi_{\mathrm{cc}})^2$, the power of the received signal is (MBB 1988):

$$P_{\mathrm{r}} = P_{\mathrm{t}} \cdot \tau \cdot \frac{A_{\mathrm{r}} A_{\mathrm{cc}}}{\Omega_{\mathrm{t}} \Omega_{\mathrm{cc}}} \cdot \frac{1}{R^4} \tag{7.45}$$

where

$P_{\mathrm{t}}$ = transmitter power;

$\tau$ = transmittance of receiver optics;

$A_{\mathrm{r}}$ = receiver optics aperture $= \frac{\pi}{4} d_{\mathrm{r}}^2$;

$A_{\mathrm{cc}}$ = corner-cube reflector area $= \frac{\pi}{4} d_{\mathrm{cc}}^2$;

$R$ = range to the target reflector;

$\Omega_{\mathrm{t}} = \frac{\pi}{4} \varphi_{\mathrm{t}}^2$;

$\varphi_{\mathrm{t}}$ = transmitted laser beam divergence;

$\Omega_{\mathrm{cc}} = \frac{\pi}{4}\varphi_{\mathrm{cc}}^2;$

$\varphi_{\mathrm{cc}}^2 = \varphi_a^2 + \varphi_b^2 + \varphi_c^2;$

$\varphi_a =$ corner-cube dihedral angle error;

$\varphi_b =$ corner-cube diffraction;

$\varphi_c = \frac{1}{R}(d_{\mathrm{t}} + 2d_{\mathrm{cc}}) =$ divergence of the return beam.

Figure 7.28 shows as an example the functional principle of a pulse radar type of laser range finder sensor. A continuous series of pulses with a high pulse repetition rate (order of kilohertz) is produced and bundled to a very narrow laser beam. The transmitted beam is deflected in the $x$- and $y$-directions by two mirrors with orthogonal axes, which can be controlled to perform various scan patterns. The rate of scan is small compared with the pulse repetition rate and the velocity of light. For a search scan covering the total rectangular FOV, the first mirror oscillates with a frequency of a few hertz, while the second one progresses slowly to start a new line when the motion of the first one returns. When the transmitted laser beam hits a corner-cube reflector on the target, it will be mirrored back toward the sensor and deflected by the mirrors into the receiver optics and compared with the outgoing signal. The range to the reflector is calculated using the time difference between the transmitted and received pulse.

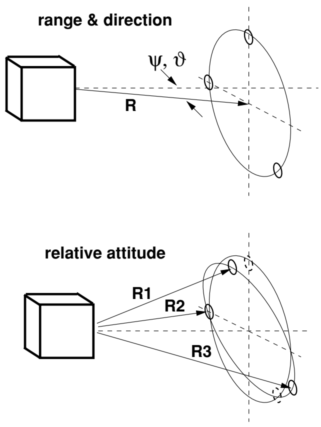


Figure 7.29. Target pattern for a laser range finder.

For the measurement of range and direction (LOS) only a single retro-reflector is necessary. Once the sensor has found the reflector, it will no longer be necessary to perform the scan over the total FOV; it will then track the reflector by scanning a narrow field around it. To increase the returning signal power, it may be useful, for very long distances, to increase the number of reflectors on the target. In this case the sensor will have to select at very short distances one of those reflectors for tracking, i.e. the most central one. Range-rate is established by differentiation (after filtering) of the range measurements.

At least three retro-reflectors will be necessary for the measurement of relative attitude (see figure 7.29). After having identified them, either by a search scan in the total FOV or by previous tracking of the complete pattern at longer ranges, the sensor will track them individually. By knowing the coordinates of the reflectors on the target and measuring the distance to each of them, the sensor can establish the angles of the coordinate frame established by them on the target. The accuracy of the relative attitude measurement is given by the distance between the reflectors and the centre of the pattern and by the range resolution of the laser range finder sensor. As the three reflectors can only be scanned sequentially, the relative motion between chaser and target would lead to relative attitude errors if their distance measurements were not propagated to the same point in time.

### Constraints due to RA measurement

The additional measurement of relative attitude will lead, however, to a number of consequences that do not exist when only range and LOS are measured.

**Limitation of useful range** The target pattern with three reflectors on a circle of a certain radius can be seen by a sensor with a certain maximum FOV only down to a certain range. For example, a sensor with a FOV of 30 deg, i.e. a half cone angle of $\psi_{\max} = 15$ deg, can see a target pattern with a radius of $r = 1$ m only down to a range of

$$R = \frac{r}{\tan\theta} = 3.75 \text{ m}$$

This phenomenon, which is inherent in the tracking of geometrical features, is also known by the term 'explosion of target in the FOV' during the approach. Unfortunately this effect cannot be compensated for by switching to a smaller target pattern, as the resolution of relative attitude will decrease with smaller target pattern if the resolution of the range measurement cannot be increased at the same time.

**Limitation of bandwidth** Since the time necessary to scan sequentially three retro-reflectors cannot be decreased below a minimum dictated by the scan mirror/motor dynamics, there will be a limitation in bandwidth of the measurements. This will also be the case not only for the relative attitude measurements but also for the range and LOS measurements, which are calculated from the same input data. The limitation of measurement bandwidth can be a problem for the overall control performance, if the GNC loop cannot observe and process the changes in the relative state between chaser and target. Such changes of the relative state can be due to the approach motion of the chaser or due to independent motion of the target.

### Range of operation and performance

**Range measurement** The typical operating range of laser range finder sensors extends from less than 1 m up to a few kilometres, depending on the measurement principle, i.e. continuous wave or pulse radar type, and on the transmitter power. The continuous wave type of laser range finders can achieve high resolution in the very short range easier than pulse type sensors, as long as an accordingly high modulation frequency has been chosen. Pulse laser types, in turn, have advantages over the continuous wave type of sensors at longer ranges. The interdependency of maximum range, resolution and wavelength for continuous wave type radars has been discussed in section 7.2.1.

**Line-of-sight measurement – field of view** The size of the FOV will be a compromise between the requirements for acquisition, trajectory control and keeping at close distance the pattern in the FOV on one side, and the necessary size, mass and power consumption for gimbals or mirrors on the other. Typical FOV values for laser range finders developed for the final approach of a rendezvous mission are of the order of $\pm$ 10–20 deg.

**Relative attitude measurement** As discussed above, the lower limit of the range in which RA can be measured is given by the FOV, i.e. up to which point all target reflectors still can be seen by the optics. It must also be taken into account that lateral and angular relative motion between chaser and target have to be covered by the sensor, so that the reflectors for RA measurement may already move out of the FOV at larger distances than indicated in the above example. The upper limit is given by the range up to which the three reflectors can be tracked separately. If one assumes that the angular distance between the reflectors needs to be of the order of 1 deg for separate tracking, RA measurement would be possible for a target pattern of the above example up to ranges of the order of 100 m. This is quite sufficient, as RA measurement is needed only in the last 20–40 m to acquire the docking axis.

**Measurement performance** Range measurement performance is determined by the limitations in time or phase resolution. For pulse type laser range finders resolutions of 5–50 mm in commercial applications and 10–30 mm in developments for space applications, are preferred. For continuous wave type laser range finders, resolutions below 1 mm can be achieved, provided the modulation frequency is high enough and, correspondingly, the wavelength is short enough. For example, with a wavelength of 10 m (3 MHz) it will not be too difficult to obtain a resolution of 1 mm; however this will be at the expense that beyond 10 m the information will be ambiguous. From the measurement principle pulse type of laser range finders the resolution of range is *a priori* not dependent on the absolute value of the range, i.e. at a range of 100 m the resolution should not be much worse than at 10 m. In reality, this is true only for the shorter ranges, as beam divergence and correspondingly decreasing signal to noise ratio will impair performance at large distances (see Eq. (7.45)). The angular resolution depends on the angular decoders of the mirror or gimbal axes. Using present technology, resolutions of 0.01 deg or better can be achieved for the above range of FOV.

### 7.4.2 Camera type of rendezvous sensor

The measurement principle of a camera type of rendezvous sensor (in some publications also called 'videometer') is based on the laws of imaging on the focal plane of a lens. With the advent of solid state charge transfer devices (CCDs and CIDs), extremely compact cameras with high resolution could be built, which opened the way for the principle of an optical camera as a solution for many sensor tasks. The basic functions of a camera sensor are shown in figure 7.30. An illuminator attached close to the optics illuminates the entire field of view of the camera. An optical pattern consisting of an arrangement of corner-cube reflectors is mounted on the target vehicle, each reflecting the received light back in the direction of the source. The image of the target pattern is read out by the CCD electronics, in which the coordinates of the reflector images are detected. Using the pattern evaluation algorithms, the information on range, LOS direction and relative attitude is computed in a data processor. The design and development of camera type RV-sensors is described in many publications, such as Bomer & Tulet (1990); MATRA (1994); Howard *et al.* (1997, 1999); Strietzel (1999).

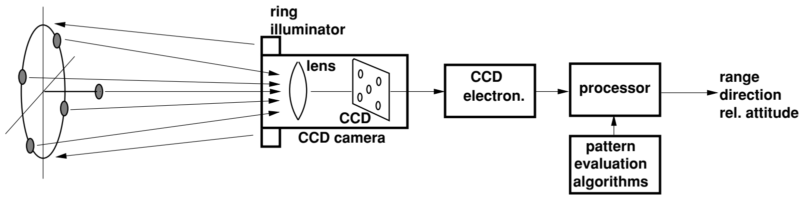


Figure 7.30. Functional principle of a camera rendezvous sensor.

The basic principle of measurement of the range $R$ from the known distance $D$ between two reflectors on the target, and from the distance $d$ of the images of those reflectors in the focal plane of the camera, is represented by the relation

$$\frac{\text{range}}{\text{distance reflectors}} = \frac{\text{focal length}}{\text{distance image points}}$$

The range is then

$$R = D \cdot \frac{f}{d} \tag{7.46}$$

where $f$ is the focal length.

The LOS angles $\phi$ and $\theta$ of a single reflector on the target vehicle can be determined from the position $x_{\text{fp}}$, $y_{\text{fp}}$ of the image of this reflector on the focal plane of the camera.

The relationship between LOS angles and imaging parameters is

$$\frac{\text{LOS angle}}{\text{FOV angle}} = \frac{\text{distance of image point from centre}}{\text{max. extension of focal plane from centre}}$$

The maximum FOV angles are $\pm\psi_{\max}$, $\pm\vartheta_{\max}$, the total field of view is

$$\text{FOV} = 2|\psi_{\max}| \times 2|\vartheta_{\max}|$$

and the total area of the focal plane is

$$A_{\text{FP}} = 2|x_{\max}| \times 2|y_{\max}|$$

The LOS angles of a reflector on the target vehicle are accordingly

$$\begin{aligned} \psi &= \psi_{\max}\frac{x_{\text{fp}}}{x_{\max}} \\ \vartheta &= \vartheta_{\max}\frac{y_{\text{fp}}}{y_{\max}} \end{aligned} \tag{7.47}$$

Since the target may have a relative attitude angle w.r.t. the camera axis on the chaser, and the projection of the pattern plane on the plane normal to the camera axis may be shortened, the measurement of the coordinates of two reflectors is not sufficient. A minimum of three reflectors is necessary to define a plane on the target. However, in many applications a configuration of four reflectors in a plane is chosen to simplify computation algorithms. The change in positions of the reflector images on the focal plane due to a relative attitude angle is a function of the cosine of this angle, which does not provide the sign of this angle. For unambiguous detection of RA an additional reflector, arranged at an out-of-plane position w.r.t. the others, is necessary. Figure 7.31 shows a typical camera target with four reflectors in-plane and one out-of-plane. The parameters, which can be obtained by evaluation of the pattern, are indicated in the figure. The evaluation steps to produce the image of the target reflectors in the camera processor are as follows.

(1) Calculation of the centre of the ellipse defined by the images of the four reflectors on the focal plane.

(2) Determination of the major and minor axes of the ellipse and the calculation of the range from the major axis, which corresponds to the diameter $D$ of the circle of the retro-reflectors.

(3) Calculation of the LOS angles from the $x$- and $y$-distances of the centre of the ellipse from the centre of the focal plane.

(4) Calculation of the pitch and yaw angles of relative attitude from the position of the image of the out-of-plane reflector on the focal plane.

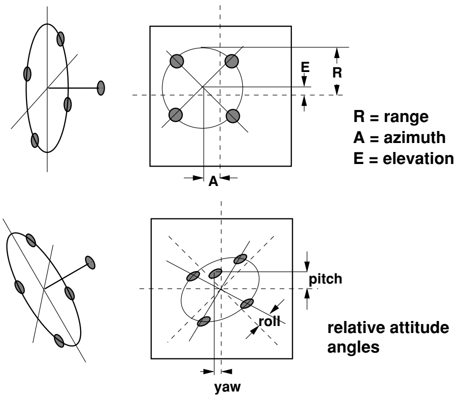


Figure 7.31. Target pattern for a camera rendezvous sensor

(5) Calculation of the roll angle from the angles of the axes of the pattern image w.r.t. the $xy$-axes of the focal plane.

The resolution of a camera is determined by the size of the FOV and by the number of pixels on the focal plane. There have been techniques developed to obtain subpixel resolution by defocusing (blurring) the image and calculating the centre of the spot from the signal strength of each pixel involved, so that the basic resolution of one pixel can be improved by a factor $\eta$. The effective resolution is then $\varepsilon_{\text{eff}} = \varepsilon \cdot \eta$. With such improvement techniques, up to an order of magnitude in resolution can be gained, i.e. the improvement factor may be $0.1 \leq \eta < 1$. The basic resolution $\varepsilon$ is

$$\text{basic resolution} = \frac{\text{size of focal plane}}{\text{number of pixels}}$$

which is, for one row or one column,

$$\varepsilon = \frac{2|x_{\max}|}{N}; \quad \varepsilon = \frac{2|x_{\max}|}{M} \tag{7.48}$$

where $N$ and $M$ are the number of pixels in a row and column, respectively. With $a$ being the diameter of 1 pixel, the size of the image of the target pattern $d$ on the focal plane expressed in numbers of pixels is given by

$$d = n \cdot a \tag{7.49}$$

Inserting these definitions into Eq. (7.46) yields the number of pixels as a function of the range:

$$n = \frac{D}{R \cdot \varepsilon} \tag{7.50}$$

which gives an indication of the development of the error with the range $R$. Considering only the basic resolution $\varepsilon$, the uncertainty of the measurement would be 1 pixel, the reciprocal value of the integer of $n$ would then be a direct measure of the range resolution. With the total FOV corresponding to a CCD of $N \times M$ pixels, the relationship between the FOV angles, $\psi_{\max}$ and $\vartheta_{\max}$, the focal length $f$ and the number of pixels in one row or one column is given by

$$x_{\max} = \tan \psi_{\max} = \frac{1}{2} \frac{N \cdot a}{f} \tag{7.51}$$

$$y_{\max} = \tan \vartheta_{\max} = \frac{1}{2} \frac{M \cdot a}{f} \tag{7.52}$$

Equation (7.50) can then be written for a row as

$$n = \frac{D}{2R} \frac{N}{\tan \psi_{\max}} \tag{7.53}$$

and for a column with $\vartheta_{\max}$ and $M$ replacing $\psi_{\max}$ and $N$ accordingly.

A particular issue for the camera type of sensor is the illumination of the target pattern. Due to the fact that the total FOV has to be illuminated for each measurement, the power density of the reflected signal is much smaller than in the case of the sharp beam of the laser range finder. For a quadratic FOV, i.e. the FOV angles are $\psi_{\max} = \vartheta_{\max}$, the half cone angle of the illuminator must be $\phi_{\mathrm{ill}} = \psi_{\max}\sqrt{2}$. The power received at the camera is, according to the radar equation,

$$P_{\mathrm{r}} = P_{\mathrm{t}} \frac{A_{\mathrm{cc}}}{A_{\mathrm{beam-ta}}} \cdot \frac{A_{\mathrm{r}}}{A_{\mathrm{beam-r}}} \tag{7.54}$$

where $P_{\mathrm{t}}$ = transmitted power; $A_{\mathrm{cc}}$ = area of corner-cube reflector; $A_{\mathrm{r}}$ = aperture of receiving optics; $A_{\mathrm{beam-ta}}$ = cross section of illumination cone at target; $A_{\mathrm{beam-r}}$ = cross section of reflected cone at receiver.

The cross section of the illumination cone at the target is

$$A_{\mathrm{beam-ta}} = \frac{\pi}{4} (R \cdot \phi_{\mathrm{ill}})^2$$

and the cross section of the reflected beam at the receiver optics is, to a good approximation, $A_{\mathrm{beam-r}} = A_{\mathrm{beam-ta}}$, which yields for the received power

$$P_{\mathrm{r}} = P_{\mathrm{t}} \frac{16 A_{\mathrm{cc}} A_{\mathrm{r}}}{\pi^2 R^4 \cdot \phi_{\mathrm{ill}}^4} \tag{7.55}$$

This result shows that the received power decreases with the fourth power of the range and of the illumination cone angle.

### Target pattern issues

As we have seen in Eq. (7.50), the resolution is a function of the ratio of target size to range. To keep the resolution at an acceptable level, the size of the pattern has to be increased with the range to be measured:

$$D = \frac{2n}{N} R \tan \psi_{\max}$$

where, e.g., the number of pixels $n$ must be 100, if a $1\%$ resolution is to be achieved. For the above example of a FOV of $\pm 10$ deg and a CCD with $1000 \times 1000$ pixels, the size of the target pattern must be 3.5 m for an operational range of 100 m in order to keep the basic resolution at $1\%$ of range. If a resolution enhancement factor $\eta$ can be applied, the size would be correspondingly smaller. In any case, the necessary distance $D$ between the reflectors increases linearly with the operational range. On the other hand, a larger target size will, in the approach, exceed already at a larger distance the available FOV of the camera. For our example of a pattern size of 3.5 m and a FOV of $\pm 10$ deg, this would happen at a range of about 10 m. Before that point, the sensor would have to switch over to a smaller pattern, to be able to continue measurements during a rendezvous approach. In order to measure down to a range of 1 m between sensor optics and target pattern, the pattern would have to be, for our example, $\leq 0.35$ m. This value has to be further reduced when lateral motions of the target have to be taken into account. As a pattern of 0.35 m diameter would, however, in our example yield a basic resolution of $1\%$ only up to a range of 10 m, a third intermediate pattern would be required to cover the range of 100 m to 1 m with a resolution of $1\%$.

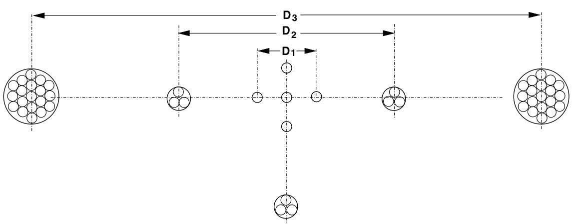


Figure 7.32. Typical target pattern set for long and short range.

The target pattern of camera type sensors will, therefore, consist of a set of concentric patterns of different sizes for the different subranges of operation. As relative attitude is required only in a range of 20–30 m, only the inner ones will have to have the out-of-plane reflector shown in figure 7.31. If the relative attitude is small, or will occur only in one known direction, it may be sufficient for longer ranges to have only two reflectors at a large distance on the target vehicle. This may be helpful for accommodation problems of the target pattern on the target vehicle. A typical set of reflector patterns is shown in figure 7.32, where the reflectors at distance $D_3$ are for the longest and the ones at distance $D_1$ for the shortest range ($D_1$, $D_2$, $D_3$ not to scale).

The second problem which affects the design of the target pattern for longer ranges is the low power density of the return signal, as has been shown above in Eq. (7.55). The operational range of a camera sensor will be limited by the signal-to-noise ratio of the reflected signal. In order to increase the power density at the camera optics, the area of the reflectors has to be increased. This leads for long range targets to the design of multi-reflector spots, as indicated in figure 7.32; these require less mass and volume than a single reflector with larger diameter.

**Range of operation and performance**

As we have seen above, the range of operation of a camera sensor is limited by the size of the target pattern and by the power density of the reflected light. The typical values for operational range and performance assume an improvement factor over the basic resolution of one pixel of $\eta$ somewhere between 1 and 10. Typical limits for a sensor with a FOV and number of pixels corresponding to the example given above would be:

range: up to 200 m with a large target pattern (cf. figure 7.32)
LOS angles: up to $\pm 10$ deg
relative attitude (pitch and yaw): up to $\pm 5$ deg
relative attitude (roll): up to $\pm 180$ deg, depending on target pattern
bandwidth: $>1$ Hz

Typical performance figures for the above example, assuming a target pattern size of 0.2 m for ranges $<30$ m and 1.5 m for ranges $>30$ m would be as follows. For range and lateral offset:

$<10$ m: $<0.01$ m
$<30$ m: $<0.1$ m
$<100$ m: $<1$ m

For LOS angles:

$<0.1$ deg

For relative attitude:

$<10$ m: $<0.5$ deg
$<30$ m: $<2$ deg

These figures are purely indicative; results of actual sensors may be better or worse, depending on design parameters and evaluation techniques applied.

## 7.4.3 Measurement environment, disturbances

**Disturbance sources**

All light sources in the FOV, in addition to the target retro-reflectors, are potential external disturbances for optical sensors. The following sources have to be considered according to the importance of their effects:

(1) the Sun;

(2) reflections of sunlight on target surfaces;

(3) reflections of sensor illuminator light on target surfaces;

(4) direct light or reflections of other light sources.

Potentially the most powerful disturbance source in the FOV of a sensor is obviously the Sun. The Sun radiates in practically all wavelengths of light so that sharp filtering of the illuminator wavelengths will not provide sufficient protection. The same is true for specular reflections of the Sun by features on the target vehicle. Specular reflection of the illuminator light is the third disturbance source which cannot be eliminated by filtering. Direct light or reflections from other sources have generally either a much lower intensity and/or have different wavelengths than the sensor illuminator. Accordingly they can be discriminated against the target reflectors by an intensity threshold or wavelength filter. In the following discussion, therefore, only the first three sources of disturbance light will be considered.

**Sensitivity of different sensors to disturbances**

**Laser range finder type** Due to the narrow beam and the very small instantaneous FOV, laser range finder types of sensors are, in their normal mode of operation, generally less sensitive to disturbances than camera type sensors. A large FOV is needed only for acquisition and in the case of a multi-target pattern, when the sensor is very close to the target vehicle. In the first case, the large FOV is needed only for a very short time; thereafter only very small areas around the reflectors are scanned. In the second case, the instantaneous FOV around a target reflector is still very small, and the three or four reflectors are distributed over a large part of the total FOV. Concerning possible disturbance by the Sun, a large part of the sensor FOV is covered in the second case by the structure of the target vehicle. Depending on the approach direction, i.e. $\pm$V-bar or $\pm$R-bar, a potential disturbance by the Sun is limited to a very short part of the approach trajectory and can, if necessary, also be excluded by operational means (e.g. change of start time of a trajectory or change of attitude for short time).

**Camera type** Camera types of sensors, because of the snapshot of the complete FOV taken at each measurement, are *a priori* more susceptible to disturbance light sources. To suppress the ‘false’ images a number of techniques can be applied, two of which are described below. Another problem for a camera type sensor is the ‘blooming’ of the CCD when an intense light source is in the FOV. In such a case, complete rows and columns of the pixels affected, and also neighbouring pixels, can become saturated, resulting in crossbars of rows and columns over the FOV, where no measurement is possible. There is not much possibility of protection against this effect in the case where one or more of the target reflectors are within these saturated crossbars. For reflectors outside the saturated rows and columns, tracking of a very narrow instantaneous FOV, similar to the technique described above for the laser range finder sensor, can be performed also on a camera image. The other pixels will, in this case, be ignored in the evaluation.

Possible protection measures against 'false' images are:

- wavelength filters on camera optics;
- subtraction of measurement with and without sensor illumination (Howard *et al.* 1999);
- flash during transfer (Bomer & Tulet 1990).

The first measure will be effective in particular against artificial light sources or reflections of such sources onto the target. As already mentioned, it will not provide protection against direct sunlight and Sun reflections. The second technique consists of a comparison of two images, one taken with and one without sensor illumination. Because the retro-reflectors of the target pattern always reflect the light back along the direction of the source, the target reflectors will be visible only on the image with sensor illumination. The third technique consists of illuminating the scene with a short flash at exactly the time when the CCD charges are transferred from the photosensitive area to the memory area. For this purpose the CCD is operated in a non-standard mode, in which the charges continuously move along the columns, i.e. a chaining of transfer phase and a clean-up phase without interruption. Permanent light sources will, therefore, affect all pixels of a column, whereas reflections from the illumination flash will create a sharp image. This special mode is called 'flash during transfer' (FDT) and is the subject of a patent by MATRA (Bomer & Tulet 1900).

None of these measures provide any protection against spurious reflections of the sensor illuminator light. This is applicable also to the laser range finder type of sensor, though in this case the illuminated instantaneous FOV is very small. Protection against spurious reflections of the illuminator light can only be obtained by proper design of the interfacing target surface and by testing of the sensor within a representative target environment (see chapter 10).

### 7.4.4 General assessment of optical sensors for rendezvous

In the very short range from a few hundred metres to capture, optical sensors provide a solution to the rendezvous navigation requirements, a solution which cannot be matched for the combination of performance, mass, power consumption and complexity by sensor systems using other measurement principles. RF-sensor techniques will require complex and bulky antennas and electronic equipment on both chaser and target vehicles to provide all the parameters. Satellite navigation, even in relative mode, will not provide performances better than $\approx$5 m for position measurement and suffers, in addition, in the very short range from shadowing of the navigation satellites by the target structure.

Concerning the operational range, camera type sensors will be limited to the 100–200 m range, whereas laser range finder types could be used up to the kilometre range, as discussed above. The choice of measurement principle is, however, more complicated and will depend also on the type of mission to be flown, i.e. whether docking or berthing, whether or not fly-arounds will be included in the last few hundred metres, whether fast target motion has to be considered in the last metres prior to capture, etc. To assess the suitability for various mission requirements, the typical advantages and disadvantages of the two sensor types will be recalled here.

### Laser range finder sensor

Advantages of a laser range finder sensor:

- Only one reflector is required on the target, if only range and LOS need to be measured.
- It has a large operational range from about 1 m to a few kilometres, depending on emitting power.
- Because of the operational principle, with its very small instantaneous FOV, the laser range finder sensor has an inherently low sensitivity w.r.t. Sun interference and other spurious light sources.

Disadvantages of a laser range finder sensor:

- This measurement principle requires moving mirrors or gimbals, resulting (a) in additional power consumption for scanning motion and (b) in reliability issues due to the sensitivity of bearings to launch and space conditions.
- Complex scan patterns for acquisition and tracking have to be performed, resulting in a limitation of bandwidth when more than a single reflector has to be scanned.
- Limitation of the minimum range, down to which relative attitude can be measured. This is due to the fact that the pattern moves out of the FOV in the last metres of approach. A reduction of the target pattern size, as in case of the camera sensor, does not help, as this would cause a corresponding increase of the measurement error.

### Camera sensor

Advantages of a camera sensor:

- There is an increase of measurement accuracy with decreasing range.
- The measurement of all navigation parameters can be obtained in one shot at the same time.

- There is a high bandwidth of measurement output, as measurement shots can be repeated at a relatively high rate.
- The relative attitude measurement can be performed down to the minimum range by using sets of smaller target patterns.
- The sensor has no moving parts and is, therefore, less sensitive to launch and orbital environment.
- Any low range can be covered in principle by adding a sufficiently small sized target pattern, which fits into the FOV at the shortest range.

Disadvantages of a camera sensor:

- For larger ranges, target reflector spots must have be at a large distance $D$ from each other and each spot may have to consist of a number of reflectors to return sufficient light (see figure 7.32). In addition, for the measurement of relative attitude in the short range, one reflector sticking out of the plane of the others is required. As a result, the accommodation of such a complex set of target patterns for short and long ranges on target spacecraft may be more difficult than that of a single pattern for the laser range finder type of sensor.
- The operating range will be limited due to the decrease of performance with the range by $1/R$ and due to the decrease of signal-to-noise ratio with the fourth power of the range and of the illumination angle.
- The FOV of this type of sensor has to be kept as small as possible due to illumination angle problems.

### Choice of sensors for RV missions

As a medium range sensor, satellite navigation in relative mode can be used in a range no closer than a few hundred metres before problems with shadowing and multi-path effects limits its usefulness. This is also the limit of the range where its performance is still sufficient for a further approach. Below this range, optical sensors are the best choice considering all relevant features and properties. Although optical sensors inherently have a limited FOV, fly-around manoeuvres can be performed with them, provided the chaser is pointing, during the fly-around manoeuvre, toward the target, and on the target side a set of multiple reflectors is mounted under different angles covering all parts of the fly-around trajectory arc.

The choice of the type of optical sensor for RV missions ending with berthing is relatively easy. As measurement of relative attitude is not necessary, the laser range finder type of sensor is the best choice. For range and LOS angle measurement, only one reflector is required, and the sensor can cover the entire short range from the order of a kilometre down to the berthing box.

For RV missions ending with docking, the choice is more difficult. Concerning the characteristics and performance required in the different ranges from a few hundred metres down to contact, a combination of laser range finder types and camera types of sensors would provide optimal performance. The laser range finder type would provide range and LOS information in the entire range, whereas the camera sensor would provide all navigation parameters, including relative attitude, with increasing accuracy in the last part of the approach, e.g. at least from approximately 30 m to docking. The penalty to be paid is a duplication of sensor heads and sensor electronics on the chaser side and the accommodation of at least two different target patterns on the target side. The accommodation problems will be increased by the fact that, due to the particular safety criticality of the last part of the approach, all sensor functions on the chaser side may have to be duplicated and operated in hot redundancy. Because of the complexity and cost of accommodation and operation of two types of sensors, spacecraft designers will of course attempt in the first instance to solve the navigation problem of the final approach with only one type of sensor. The following criteria may play a role in the choice of sensor type.

- If a medium range sensor, i.e. satellite navigation or any other type, can be used down to less than 200 m, the use of a camera sensor only may become possible for the short range and may satisfy all requirements. In this case a very large target pattern for the 100–200 m range would have to be accommodated on the target.
- If the medium range sensor ceases to be useful at ranges larger than 200 m, the laser range finder type is the better choice. This type of sensor may cause difficulties, however, in the very short range concerning the measurement of relative attitude, when the target pattern is moving out of the FOV. It may also cause problems due to the limited bandwidth with which the navigation information is provided, when three reflectors have to be scanned for relative attitude measurements. The possibility of using a laser range finder sensor only, including the short range of approach, will depend, therefore, on the motion characteristics of the target.
- A combination of both types of sensors may have to be used if (a) the target attitude motion has amplitudes which would use up a significant part of the reception range of the docking port, if (b) the cycle time of the attitude motion is shorter than the residual approach duration after loss of relative attitude (see above) and if (c) the medium range sensor cannot be used at ranges closer than a few hundred metres.

These considerations can of course only indicate the issues directly connected to the measurement principles. In a spacecraft project, other design and operational constraints may also eventually determine the choice.